Impact of animal burrows on earthen levee body vulnerability to seepage

Impact of animal burrows on earthen levee body vulnerability to seepage

Article *in* Journal of Flood Risk Management · August 2019

DOI: 10.1111/jfr3.12559

CITATIONS
0

READS
79

5 authors, including:

Silvia Barbetta
Italian National Research Council
57 PUBLICATIONS **521** CITATIONS
SEE PROFILE

Stefania Camici
Italian National Research Council
48 PUBLICATIONS **438** CITATIONS
SEE PROFILE

Pierluigi Claps
Politecnico di Torino
118 PUBLICATIONS **1,775** CITATIONS
SEE PROFILE

T. Moramarco
Italian National Research Council
251 PUBLICATIONS **5,297** CITATIONS
SEE PROFILE

Impact of animal burrows on earthen levee body vulnerability to seepage

Michela Rosa Palladino[1], Silvia Barbetta[2], Stefania Camici[2], Pierluigi Claps[1] and Tommaso Moramarco[2]

(1) *Politecnico di Torino, Corso Duca degli Abruzzi 24, Torino, Italy.*

(2) *National Research Council, IRPI, Via Madonna Alta 126, Perugia, Italy.*

Abstract: A novel procedure for estimation of the vulnerability to seepage inducing piping processes in earthen levees affected by animal burrows is presented. The proposed methodology combines an available procedure of seepage vulnerability assessment for undamaged levees with the result of a finite element analysis software, which is used for identifying the seepage path and hydraulics head profile of both damaged and undamaged levees. The main steps of the procedure for estimating the impact of burrows in increasing the vulnerability of levees are presented. Twenty-one levees along the Tanaro River (north-western Italy) are used as a case study, and the results show that the critical conditions for the onset of inner erosion are achieved for shorter flood durations in damaged levees. If burrows occur, the probability of inner erosion (seepage probability) increases resulting in a potential increase of forming longer tunnels. This approach is a first attempt to quantify the seepage probability of extended levee systems affected by burrows and is applied for simplified geometrical and two-dimensional representation of the cavities. This procedure

This article has been accepted for publication and undergone full peer review but has not been through the copyediting, typesetting, pagination and proofreading process which may lead to differences between this version and the Version of Record. Please cite this article as doi: 10.1111/jfr3.12559

can be applied by the hydraulic Authorities to set the priorities in levees maintenance. Future research would focus on the analysis of more realistic burrows conditions.

Keywords: Levee failure, piping, seepage, vulnerability index, damaged levee, animal burrows.

1 INTRODUCTION

Floods are among the most widespread and destructive environmental hazards worldwide and different protection measures are implemented to reduce their impact. Properly designed earthen levees represent a common structural measure to reduce the hydraulic risk in floodplains. However, possible damages to the levee system can compromise its efficacy (*ASCE, 2011; ICOLD, 2013*) and induce a 'residual risk' to be taken into consideration to avoid flood risk underestimation (*Ludy and Kondolf, 2012*).

According to the available statistics, overtopping is the most prevalent failure mechanism of earthen levees worldwide (*Nagy and Toth, 2005; Costa, 1985*). However, other processes can also endanger the functionality of the levees. (*Ojha et al., 2001; Serre et al., 2008; Sills et al., 2008; Huang et al., 2014*). Among them, the seepage-induced piping phenomenon in the levee body, henceforth, referred to as "seepage processes" or "inner erosion" or "piping", has received much attention due to frequent occurrence in the recent past leading to significant damages. The seepage process is initiated by the hydraulic gradients established between the riverside and the landside slopes of the embankment resulting in removal of fines soil particles, along the seepage path. As the seepage process

evolves, the resistance of the granular material to internal erosion decreases and thereby resulting in displacing larger sediment particles leading to rapid formation of large pipes. The outer portion of the embankment would appear to remain almost undamaged even when the structure is close to the failure condition. This suggests that the inner erosion can remain undetected making the failure scenario barely predictable and, hence, resulting in catastrophic failure (*Wu et al., 2011; ICOLD, 2013; Danka and Zhang, 2015*). Various methods have been proposed in the literature to simulate the seepage and to identify the location of the saturation line (*Van Iterson, 1917; Kozeny, 1931; Casagrande, 1937; Bardet and Tobita, 2002*). Notwithstanding the accuracy of these methods, the difficult estimation of the geotechnical/hydraulic parameters makes their application feasible only for isolated and well-known case studies. Therefore, the development of expeditious procedures which enable the identification of the most vulnerable levees, within extended the systems, appears to be a desirable solution at catchment scale.

With this objective Vorogushyn et al. (*2009*) outlined a procedure for seepage vulnerability assessment, based on a probabilistic approach and a fragility curves estimation approach. Mazzoleni et al. (*2015*) suggested a method for assessing the flooding residual hazard due to piping-induced levees failures, based on the failure probability computed through the Hazard Factor and the Hydraulic Gradient. To assess the levee vulnerable to seepage, Michelazzo et al. (*2018*) proposed a Vulnerability Index defined as the ratio between the expected persistence of the flood and the minimum time necessary for the phreatic line to emerge along the landside slope of the levee, called critical time.

Camici et al. (*2017*) developed a practical procedure that enables the definition of the levee body vulnerability to seepage, once the hydraulic/geometric characteristics are defined. This method, recently enhanced by Barbetta et al. (*2017*), accounts for the uncertainty in the estimate of soil hydraulic conductivity through a probabilistic approach.

The above approaches generally assume the levees to be intact and homogeneous. However, natural degradation processes and the activity of wild animals can often compromise the structural integrity. In the last years, several levee management boards and maintenance agencies worldwide have reported information on earthen levee breaches related to the activity of animals (*FEMA, 2005; Bayoumi and Meguid, 2011; Camici et al., 2017; Orlandini et al., 2015; Saghaee et al., 2012*). The main effect is the removal of loose materials along the slopes and from the core of these structures resulting in modifications of both the external and the internal geometry. These modifications reduce the strength characteristics and alter the hydraulic configuration (*FEMA, 2005*) of these structures.

To tackle this problem, the present study proposes a new procedure to assess the variation in seepage vulnerability induced in earthen levees by the presence of burrows, here represented through a simplified geometry. The method is based on two main steps: 1) the levee body vulnerability to seepage is first assessed for undamaged levees through the approach by Barbetta et al. (*2017*); 2) the impact of burrows is investigated by analysing its effect on the seepage flow, by a 2-dimensional (2D) numerical model SEEP/W (GEOSTUDIO® 2012 Office). The choice to adopt a 2D model was essentially made to reduce the computation time, that is particularly long for 3-dimensional (3D) simulations (*Jafarzadeh et al., 2009*; *Taccari, 2015*; *Cheng et al., 2016*). Furthermore, the analysis

reveals that when the flow is reasonably parallel to the levee cross section which is acceptable when simple burrow configurations are considered, the 3D and 2D models compare favourably (*Cheng et al., 2016*), thus fostering the use of 2D models. Finally, the adoption of a 2D model is deemed acceptable for a screening-level analysis (*Cheng et al., 2016*) and, therefore, it is considered coherent with the objectives of this study intended as a first step in the development of a more accurate procedure to enable the assessment of the impact of burrows formed in earthen levees of more complex geometries. Moreover, such procedure would enable us to identify the failure susceptible levees of embanked river stretches which requires urgent attention with regard to inspections, monitoring and more accurate analyses.

The procedure characterizes the burrows effect by identifying the flood duration so that a damaged levee reaches same hydraulic critical conditions of the undamaged one and it is applied to the Tanaro River levee system, in north-western Italy, where 21 earthen levee stretches are selected as a case study. The paper is organized as follows: Section 2 describes the expeditious procedure for seepage vulnerability assessment of undamaged levees (*Barbetta et al.,2017*) and presents the new procedure for quantifying the impact of burrows. Section 3 gives details of the case study and the data used. Section 4 presents the results and Section 5 outlines the final conclusions.

2 METHODOLOGY

2.1 Undamaged earthen levees: expeditious procedure for seepage vulnerability assessment

The procedure proposed by Barbetta et al. (*2017*) assumes the emergence of the phreatic line at the landside slope as the necessary condition for the onset of inner erosion through the levee body (*Vorogushyn et al., 2009*). Therefore, inner erosion is not considered until the saturation line crosses the base of the embankment (solid blue line in *Figure 1*).

The levee vulnerability to possible piping is simply assessed by comparing the distance at which the seepage line intercepts the ground level, i.e., the maximum length of the seepage line (x_{max} in *Figure 1*), with the width of the landward portion of the levee base (segment $\overline{AB}$ in *Figure 1*): the structure is safe as long as $\overline{AB}$ exceeds x_{max}. Conversely, the critical condition (dashed red line in *Figure 1*) is achieved as the seepage line intercepts the outer toe of the levee (point B in *Figure 1*), i.e. $x_{max} = \overline{AB}$. The estimate of x_{max} is based on the analytical solution of the seepage flow proposed by Marchi (*1961*). The spatial variation of the saturation line (see *Figure 1*) above the groundwater table, *H(x)*, is formulated by:

$$H(x) = h_0\left[1 - erf\left(\frac{x}{2\sqrt{\frac{\xi}{K_s \cdot H_0 \cdot D}}}\right)\right] \qquad (1)$$

with h_0, the hydraulic head in the channel above the groundwater table; K_s the hydraulic conductivity; ξ, the porosity of the soil; H_0, the thickness of the aquifer; D the flood duration; and *erf* represents the error function, i.e. twice the integral of the Gaussian distribution with zero mean and variance equal to 0.5.

Camici et al. (*2017*) used a dimensionless coordinate system with axes $x^*=x/L$ and $h^*=h/H_s$, with H_s=height of the levee top above the ground level and L=horizontal distance between the inner top of the levee and the external levee toe. Focusing on the seepage through the levee body alone, these authors derived a dimensionless formulation as:

$$h^*(x^*) = \frac{h_0'}{H_s} \cdot \left[1 - erf\left(\frac{x^*}{2\sqrt{K_s \cdot \delta}} \right) \right] \quad (2)$$

where $\delta = \frac{H_0 \cdot D}{L^2 \cdot \xi}$, and $h_0' = (h_0 - a)$ is the water level above the river bed, with a =depth of the groundwater table from the river bed (*Figure 1*). Finally, x^*_{max} is obtained by imposing that $h^*(x^*)$ is equal to zero:

$$\frac{h_0'}{H_s} \cdot \left[1 - erf\left(\frac{x^*_{max}}{2\sqrt{K_s \cdot \delta}} \right) \right] = 0 \quad (3)$$

If the saturation line is embedded in the levee body, i.e. $x^*_{max} < \overline{AB}^* \left(\overline{AB}^* = \frac{\overline{AB}}{L} \right)$, piping condition is avoided; otherwise, if $x^*_{max} \geq \overline{AB}^*$, the seepage condition within the levee body would enable the piping and the levee is considered vulnerable to internal erosion.

The vulnerability of the levee is finally quantified through the Vulnerability Index, I_{Vseep}, defined as (*Barbetta et al., 2017*):

$$I_{Vseep} = \frac{x_{\max}^* - (1 + x'^*)}{x_{\max}^*} \quad (4)$$

with $x'^* = cot(\alpha)\left(1 - \frac{h_0'}{H_s}\right)$ and α=waterside slope of the levee (*Figure 1*).

If I_{Vseep}<0, the seepage line is embedded into the levee body, then the structure is safe; if I_{Vseep}=0, the seepage line crosses the landside levee toe, marking the threshold condition for the onset of seepage; if I_{Vseep}>0, the seepage line intercepts the landside slope and the structure is exposed to seepage.

Among the variables that determine I_{Vseep}, the geotechnical parameters K_s and ξ are characterized by relevant uncertainties. Therefore, Barbetta et al. (*2017*) adopted a probabilistic approach based on the definition of the probability distributions of the geotechnical variables. Since the position of the seepage line is more sensitive to K_s than ξ (*Vorogushyn et al., 2009; Barbetta et al., 2017*), the variability of ξ is neglected and the 'fragility curves' (*Apel et al., 2008; Vorogushyn, 2009; Schultz et al., 2010*) are drawn considering the variability of K_s alone (*Figure 2*). In *Figure 2a*, the fragility curves show the relationship between I_{Vseep} and K_s for different δ values, i.e., for different flood wave durations, and for a fixed ratio h_0' / H_s. Subsequently, the probability distribution of I_{Vseep} is identified for any fragility curve (see *Figure 2b*), allowing us to define for different flood durations (D=12, 24 and 48 hours), the levee seepage probability, P_{seep}, as the complementary to 1 of the cumulative probability for I_{Vseep}=0. Based on the values of P_{seep}, Barbetta et al. (*2017*) also suggest a possible ranking for the levee seepage vulnerability (*Table 1*). Currently, the thresholds are heuristically defined, but they could be upgraded based on historical failure data.

2.2 Damaged earthen levees: impact of animal burrows on the seepage vulnerability

The adverse impact of burrows on the levee seepage probability is mainly related to the hydraulic alteration (*FEMA, 2005*) and, specifically, to the considerable reduction of the saturation time of the damaged levee in comparison with the undamaged one (*Cobos Roa, 2015*).

It follows that, given the flood water level (h_0'), the hydraulic head distribution achieved in the undamaged levee for a generic flood duration, D, is reached in the damaged levee for a

shorter duration, henceforth, referred to as "the equivalent duration", D_{eq}. Analogously, the hydraulic head distribution associated with the critical condition, i.e., the interception of the levee toe by the saturation line, is reached faster in the damaged levee than that in the undamaged one. Therefore, the presence of the burrows reduces the flood critical duration of the undamaged levee, referred to as D_c, and the damaged levee is vulnerable to seepage for a flood duration shorter than D_c, henceforth referred herein as "equivalent critical duration", $D_{c,eq}$ ($<D_c$). Obviously, $D_{c,eq}$ is not critical for the undamaged levee while it is critical for the damaged one, and the damaged levee is then expected to be characterized by a higher vulnerability than the intact structure.

This study presents the basic ideas of the new procedure addressing the quantification of the seepage probability variation due to burrows, named ΔP_{seep}. This procedure identifies the main steps to understand the level of vulnerability increase of an undamaged levee due to the presence of burrows. The method is based on coupling of the expeditious procedure developed by Camici et al. (*2017*) with the outcomes of a 2D finite element analysis software. The main concepts of the methodology, based on six major steps, are described in the following subsection.

2.2.1 Solution procedure

1. The seepage probability of the undamaged levee, P_c, with known geometry (L, H_s and α) is computed, for a flood duration D, through the expeditious procedure by Barbetta et al. (*2017*), for the known values of maximum water level, h_0', thickness of the aquifer, H_0, and flood duration, $D=T$ *hours*. Specifically, the procedure assumes a constant water level for the duration D.

2. The undamaged levee is modelled with the use of a Finite Element Model (FEM) (*Figure 3a*): SEEP/W by GEOSTUDIO® 2012 Office. The model solves the 2D Richards equation for unsaturated flow in porous media and computes the hydraulic head distribution within the seepage domain in transient conditions. The hydraulic head distribution is evaluated for different time steps in the interval 0÷T hours (T is the expected flood duration, *D*, measured in hours, for the undamaged structure) (*Figure 3b*).
3. The presence of a burrow in the levee body is simulated in SEEP/W (*Figure 4a*) by a tunnel having a soil layer with high permeability. Under the same boundary conditions adopted in step 2, the hydraulic head distribution is computed for the damaged levee (*Figure 4b*), for different time steps in the interval 0÷T hours.
4. The hydraulic head profiles obtained with SEEP/W at the vertical section crossing the centreline of the levee (section a-a' in *Figures 3a* and *4a*) are compared for different time steps and for both the undamaged and damaged structures. The equivalent critical flood duration, $D_{c,eq}$, is identified (see *Figure 5* where D_c=24 hours) as the duration for which at centreline line of the damaged levee is achieved, on average, the same hydraulic head of the undamaged one for $D=D_c$.
5. Considering that the seepage probability of the damaged levee for a flood duration $D_{c,eq}$ is the same as that of the undamaged one for a duration $D_{c,}$ as shown in *Figure 6*, the new origin of I_{Vseep} axis for the damaged levee is identified. This is located by the intercept of the vertical line through the point lying on the fragility curve with $D_{c,eq}$, and corresponding to the same vulnerability of the undamaged levee, with the I_{Vseep} axis. In

other words, the new origin of I_{Vseep} axis is found by shifting the old origin, according to the horizontal distance between the two I_{Vseep} for the duration of D_c (I_{Vseep}=0) and $D_{c,eq}$ (I_{Vseep}=-3.6) corresponding to the two undamaged levee fragility curves having the same seepage probability. In this way, the seepage probability of the damaged levee, $P_{c,eq}$, for the duration D_c can be assessed and, as shown in *Figure 6*, it is equal to 75%, with an increase, ΔP_{seep}, of 45% with respect to that of the undamaged levee (30%). Therefore, *Figure 6* shows the fragility curves referring to the seepage probabilities of the undamaged levee for flood durations $D_{c,eq}$ (red) and D_c (blue), respectively.

6. Finally, the seepage probability variation due to the presence of burrow is computed as (*Figure 6*):

$$\Delta P_{seep} = P_{c,eq} - P_c \quad (5)$$

It is worth noting that the geometry of burrows adopted for the analysis is a simplified representation of the actual burrows characterized by wide variability of shape, position and size. Nevertheless, the analysis can be considered as a sound tool for identifying the embanked river stretches where inspections, monitoring and more accurate studies can be promoted.

3 CASE STUDY AND DATASET

The study is performed on the levee system of the Tanaro River (north-western Italy), one of the main tributaries of the Po River, with a drainage basin of 7956 km^2 (*Figure 7*). The catchment includes both Alpine (in the northern sector) and Apennine (in the southern portion) watersheds, characterized by prevailing spring-summer and spring-fall floods, respectively.

The main urban settlements are located in the middle-lower basin and are nearer to the river. The towns of Alessandria, Asti, Alba and Ceva are frequently affected by severe floods and, hence, are identified as critical hydraulic points (*Figure 7*). To select the homogeneous levee stretches, numerous cross sections are extracted from a high-resolution Digital Terrain Model (DTM) (1-meter resolution). Twenty-one homogeneous levee stretches are identified; the geometric characteristics and the water level data (H_{200}) corresponding to a 200 years flood are summarized in *Table 2*. The overall length of the selected levee system is 8.2 Km and it is located in the neighbourhood of the urbanized areas. The seepage probability estimate is carried out for 15 levees whose crest level, H_s, is higher than H_{200}, thus excluding 6 overtopped levees (*Table 2*).

Appendix A provides a list of the data sources used in the present study.

4 RESULTS AND DISCUSSION

4.1 Seepage vulnerability of undamaged earthen levees

The seepage vulnerability is first estimated for the undamaged levees through the expeditious procedure formulated by Barbetta et al. (*2017*). The required geometric features (H_s, α and L) are obtained through the DTM. Based on the available information (see Appendix A), an average value of 15 m for the thickness of the aquifer, H_0, was estimated in the study area.

Following the sensitivity analysis carried out by Barbetta et al. (*2017*), ξ is considered as a constant equal to 0.1, and the uncertainty in K_s is addressed by randomly generating 10000 K_s values, in the wide range $\underline{10^{-9} \div 10^{-3}}$ ms^{-1}. It is assumed that the variable K_s follows the

log-normal distribution with mean $\mu_{Ks}=10^{-5}$ ms^{-1} and standard deviation $\sigma_{Ks}=25\mu_{Ks}$ (*Vorogushyn et al., 2009*). For each levee, water levels corresponding to the 200-years return period, H_{200}, are available for the three durations: D=12, 24 and 48 hours. The three vulnerability classes identified by Barbetta et al. (*2017*) are used for the classification (*Table 1*). The results for undamaged levees are summarized in *Table 2* and *Figure 8* where the number of levees belonging to each vulnerability class is reported as a percentage of the whole dataset (21 levees).

The seepage probability increases with the flood duration. For D=12 hours, 10 out of 21 levees (47% of the total) are characterised by Low vulnerability and 5 levees (24% of the total) by Medium vulnerability. When D increases up to 24 hours, 47% of the levees are found characterised by Medium vulnerability and 24% by Low vulnerability. Finally, for D=48 hours, 2 levees (9% of the total) become highly vulnerable, while 12 levees (57%) and one levee (5%) are characterized by Medium and Low vulnerability, respectively.

4.2 Seepage vulnerability of damaged earthen levees

To define the seepage probability variation induced by the burrows, ΔP_{seep}, the equivalent critical duration, $D_{c,eq}$, is first identified by comparing the hydraulic head profiles of the undamaged and damaged levees during the time-interval corresponding to the duration D.

4.2.1 Model setting in SEEP/W

To compare the hydraulic head profiles in the undamaged and damaged levees, each homogeneous levee is modelled in SEEP/W. At the beginning of the simulations, the seepage domain is assumed to be in stationary conditions, with the water level h_0'=0 m.

Hence, according to the hypotheses of Marchi (*1961*), a rectangular flood hydrograph with $h_0'=H_{200}$ is simulated in the river channel considering a constant water level condition during the flood. This schematization is considered suitable for the objectives of the study since it provides a solution that errs on the side of caution as the analysed wave represents the envelope of all possible hydrographs that are expected to pass the river reach protected by the levee (*Marchi, 1961*). Transient conditions are considered in order to analyse the temporal evolution of the hydraulic heads in the levee body during the flood. Since simulating with SEEP/W is very time-consuming, only the duration equal to 24 hours, relevant for the study area, is considered.

The levee geometry is reproduced in SEEP/W along with the width of the foundation and the piezometric level below the ground surface, *a*, which was not analysed in the expeditious procedure (*Figure 1*). The foundation width is defined considering the information derived from the water table map: the foundation is extended laterally, beyond the levee footprint, for 100m towards the waterside and for 300m towards the landside. The foundation is assumed delimited at the bottom by a layer of impervious soil, excluded from the computations. The piezometric level, *a*, is provided by the water table depth map of the study area (variability range: 0÷10 m).

To solve the seepage equation, SEEP/W requires the univocal definition of the geotechnical parameters: the hydraulic conductivity in saturated, K_s, and unsaturated, $K_{s,u}$, conditions, the coefficient of volumetric compressibility, m_v, and the saturated and residual volumetric water contents, θ_s and θ_r, of the materials which make up the levee body and the foundation. Since an accurate geotechnical characterization is not possible, the levee and

the foundation are assumed to be composed of the same, homogeneous and isotropic material. The soil classes of this material are derived from the literature on the basis of the saturated hydraulic conductivity of the levee-foundation system selected in the range of variation $\underline{K_s=10^{-9}\div10^{-3}}$ ms^{-1} (*Yu et al., 2015)* as shown in *Table 3*. Based on the soil classification, the remaining geotechnical parameters are also derived. The values of θ_s and θ_r can be deduced by Tuller and Or (*2004*) for different textural classes (*Table 4*), whereas, m_v can be derived by Domenico and Mifflin (*1965*) (*Table 5*). The geometrical (H_0 and a) and geotechnical (K_s, θ_r, θ_s and m_v) parameters to be used in the FEM analysis are defined within the variation ranges (*Table 6*) due to limited information on the seepage domain. Since unique values are needed, a sensitivity analysis is performed to define the key parameters: first, the possible ranges of variation of each of the four parameters (K_s, m_v, a and H_0) are identified; second, several simulations are run, keeping three out of the four parameters as constant and varying the value of the fourth one.

The results of the analysis indicate that the position of the seepage line is highly sensitive to K_s (*Figure 9a*) and m_v (*Figure 9b*) which need to be carefully defined. Conversely, the seepage line is slightly sensitive to the values of a (*Figure 9c*) and H_0 (*Figure 9d*) that are assumed to be constants: a is established at 5 m, equal to the average value in the study area and H_0 is established at 15 m, adopting the same value for the expeditious procedure and corresponding to the mean value of the study area. It is worth noting that the effect of a value on the location of the seepage line depends also on the groundwater width that, for the investigated case study, was derived from the water table depth map of the Piedmont Region. Therefore, the sensitivity analysis for different values of the water table depth must

be carried out when different configurations of the groundwater characterize the selected study area.

On this basis and in order to recreate in the SEEP/W model the same conditions adopted in the expeditious procedure, the 2D-hydraulic numerical model setting is implemented for the undamaged levee. The hydraulic conductivity of the levee-foundation system is assumed equal to the critical hydraulic conductivity, $K_{s,c}$, that provides I_{Vseep}=0 for D_c=24 hours. Once $K_{s,c}$ is identified, it allows the classification of the earth fill material of the levee and foundation (as a clay, silt or sand). Based on this classification, θ_s and θ_r and the range of variation of m_v are identified: m_v value is calibrated by varying this parameter to get the best fit between the seepage line deduced from Marchi formulation (*1961*) (black dashed line in *Figure 10*) and the seepage line of SEEP/W model (coloured solid lines in *Figure 10*).

When all the parameters are identified, the damaged embankment is modelled using the SEEP/W model. The burrows are simulated through soil layers with high hydraulic conductivity, $K_{s,b}$, the value of which is deduced from the literature and assumed equal to 1 ms^{-1} (*Cobos Roa, 2015*).

Considering that the actual geometry of the burrows can be very complex (*Borgatti et al., 2017*), this study is mainly addressed to define a general procedure based on a simple 2D configuration of burrows that has the potential to be enhanced by using more complex burrow configurations. For this reason, the discontinuities are assumed as horizontal, cylindrical of size 10 cm diameter, that reduce to rectangular shapes in 2D analyses. The diameter of the cavity is defined based on the evidences from field surveys carried out by

the authors themselves and verified from the literature. Accordingly, the value of 10 cm is assigned as the size of small burrows, such as the ones dug by little ground squirrels (typical diameter 5-25 cm, according to *Bayoumi and Meguid, 2011*) or crayfishes (4-7 cm, according to *Bendoni et al., 2016*) which can severely compromise the integrity of the levees.

The burrows are supposed to be located at the riverside, a quite common configuration in real cases (*Chlaib et al., 2014*). Different locations and lengths are analysed: the level of the burrow, h_b, is varied from 1/6 (burrow A) to 1/2 (burrow B) and 5/6 (burrow C), the height *Hs* (*Figure 11a*). Moreover, the burrow length, L_b, is varied from 1/4 to 1/2 and 3/4 the width of the levee measured at the location of the burrow, $L_s(h_b)$. Overall, 9 different configurations are analysed for each of the levees.

4.2.2 Vulnerability Analysis

The simulations of SEEP/W show that the presence of the burrows extends the saturation zone in the levee body and that the seepage line moves progressively towards the landside slope as the length of the burrow increases. Such a situation is depicted in *Figure 12*, showing the seepage lines in the levee Ta_07_dx, for D_c=24 hours along with different levels and length of the burrow (burrow A, B and C in panels *12a*, *12b* and *12c*, respectively). The comparison of the total head profiles which develop in the centreline of the damaged and undamaged levees in the 24-hours interval allows us to identify the equivalent critical durations, $D_{c,eq}$ (*Figure 13*). The results obtained for all the levees highlight that the flood duration necessary for the onset of the seepage is drastically reduced in the damaged structures. *Figure 13* shows that the critical duration for the

triggering of piping decreases from 24 hours (undamaged structure) to 19 hours (damaged) and becomes even shorter (0.5 hours) if the levee is severely damaged. If we focus on a specific location of the burrow (A, B or C) and analyse the effect of the length, we observe that $D_{c,eq}$ reduces as the length increases. Conversely, if the length is kept constant and different locations are compared, it is not possible to highlight a general trend. By way of example, the results for the levee Ta_07_dx show that for L_b=1/4L_s(h_b), $D_{c,eq}$ reduces as the burrow moves towards the crest of the levee. When higher lengths are examined (L_b=1/2L_s(h_b) or L_b=3/4L_s(h_b)), $D_{c,eq}$ reduces for burrows located at lower levels. Considering the whole dataset and estimating the maximum and minimum equivalent critical duration for each configuration, it is confirmed that for an established elevation of the burrow (A or B or C), $D_{c,eq}$ constantly decreases for increasing lengths (see *Table 7*). Conversely, if a specific burrow length is analysed, results do not identify a tendency for an increase or decrease of the $D_{c,eq}$ if the burrow moves vertically within the levee. It's worth noting that the C burrow configuration is analysed only for 6 levees out of 15 i.e., for the remaining 9 embankments, the water level does not reach the higher tunnel. The estimation of $D_{c,eq}$ allows us to identify the fragility curves for assessing the increase of the seepage probability for the damaged levee as shown in *Figure 14* for Ta_07_dx levee. As it can be seen, as $D_{c,eq}$ decreases, the variation of seepage probability, ΔP_{seep}, increases. In addition, the augmentation of ΔP_{seep} is also found increasing with the length of the burrow. Specifically, with ΔP_{seep} varying between 3.9 and 11.4% for the shortest burrow, the percentage variation of the seepage probability rises in the ranges of 22.7÷37.0% for L_b=1/2L_s(h_b), and 27.0÷50.9% for L_b=3/4L_s(h_b). Instead, keeping the length of the burrow

constant and varying its position in height, a specific trend for ΔP_{seep} is not found (see *Figure 15*); whereas for L_b=¼L_s(h_b), the burrow C induces the highest variation in ΔP_{seep}=11.4%, versus 6.6% associated with burrow B and 3.9% associated with burrow A. For the other lengths, the magnitude of ΔP_{seep} is inverted (*Figure 15*).

The results obtained for all the levees, and for different locations and lengths, indicate that the burrows induce a variation of the seepage probability between 2.0% and 55.2%, with ΔP_{seep} increasing as the length of the cavity increases (*Figure 16*). Specifically, for lengths varying from 1/4, to 1/2 and 3/4L_s(h_b), the minimum ΔP_{seep} increases from 2.0% to 21.3% and 31.0%, respectively, whereas the maximum ΔP_{seep} changes from 19.3% (1/4L_s(h_b)) to 55.2% (1/2L_s(h_b) and 3/4L_s(h_b)). Conversely, a monotonically increasing/decreasing relationship between the burrow location and the seepage probability modification cannot be found and further investigations are required. *Figure 16* summarizes the results for the investigated levees: ΔP_{seep} values are shown as dots along with the 5th, 50th and 95th percentiles. Moreover, the 50th percentiles computed for all the burrow locations are compared in *Figure 16d*.

Results are also summarized in *Table 8* in terms of vulnerability classes of the levees for different locations and lengths of the burrows. The presence of the burrow can entail a shift from a lower to a higher vulnerability class. As the burrow C is higher than the water level for 9 levees out of 15, its presence is irrelevant, and no results are provided in *Table 8*.

The levees distribution in the vulnerability classes is illustrated in *Figure 17* for both the undamaged and damaged embankments. For the shortest length of burrow, the percentage of levees with a medium vulnerability increases from 67% (no burrows) up to 80%, 93%

and 100% when burrows A, B and C are considered, respectively, while no high vulnerability of levees is identified. For L_b=1/2L_s, a significant change of the distribution classes is identified, with 100% and 93% of the levees characterized by high vulnerability for burrow A and B, respectively. Moreover, all 6 levees investigated for burrow C configuration belong to the high-vulnerability class. Similar comments hold when the longest burrow is simulated. *Figure 17* clearly shows that for all the examined locations (A, B and C), the percentage of levees falling in progressively higher vulnerability classes tends to augment as the length of burrows increases. This result confirms the role exerted by the length of the tunnel in the definition of the seepage vulnerability class. Conversely, when the burrow location is investigated, a monotonically increasing/decreasing relationship between the position and the effect on the seepage vulnerability cannot be found, probably due to the range of vulnerability classes, which could be refined using historical levee collapses.

5 CONCLUSIONS

A new procedure for the estimation of the impact of animal burrows on the seepage vulnerability of earthen levees is presented in this work. The proposed approach is intended as a first step in the development of a more accurate operational procedure able to assess the impact of the burrows also considering more complex geometries through practical and reliable tools ("vulnerability increase diagrams"). The study presents the basic ideas of a new approach to quantify the seepage probability variation due to the presence of burrows and presents the results achieved by considering a simplified and two-dimensional burrows geometry. Specifically, the analysis quantifies the effect of horizontal burrows

characterized by different locations and lengths. The novelty of the proposed approach comes from the coupling of an available expeditious procedure for the estimation of the seepage probability for undamaged levees (*Barbetta et al., 2017*) with a 2D numerical model (SEEP/W by GEOSTUDIO® 2012 Office) employed for identifying the seepage paths and the hydraulic head profiles in the levee, with and without burrows.

Based on the database of 15 earthen levees selected along the Tanaro River, north-western Italy, the fundamental role of the flood duration in the seepage vulnerability of undamaged levees is proved. As the flood duration increases, a significant percentage of levees moves from the lower to the higher vulnerability classes. When the impact of the burrows is analysed, a generalised worsening of the stability conditions emerges due to a fast saturation of the embankments, which reduces the critical onset duration of the levee, i.e., the time required for the saturation line to reach the landside toe, a configuration which marks the onset of the piping. Therefore, it is found that the geometry adopted for representing burrows significantly, affects the reduction of the equivalent critical duration by increasing the vulnerability to seepage of levees.

Notwithstanding the interesting results achieved, it is worth noting that the geometrical simplification of the burrows may be a limitation of the proposed approach, considering that burrows in reality may have arbitrary shapes and may extend in different directions. Indeed, geometrical structures of burrows in levees may significantly vary according to the species of wild animals. For instance, porcupines (foxes, badgers, etc.) dig the burrows generally at mid height of levees, making long tunnels of different shape and direction (*Camici et al., 2017*). Differently, the coypus dig at baseflow level with tunnels moving at

the same level. So, identifying the actual geometry of tunnels in levees without an accurate 3D tomography of the embankment is really tedious and uncertain, and this explains the choice of a simplified configuration of burrows in this study. However, the choice to adopt a simple geometry allowed us to understand the saturation spreading process, if different tunnels are located in the embankment. Indeed, the study proves that the presence of burrows reduces the 'critical time' of saturation for the levee and thereby, inducing the collapse of a levee even for flood durations shorter than the critical time of undamaged levees. Of course, these results hold only under the assumptions made within the study which may not be applicable for different geometries of burrows. However, the method may yield precautionary results under real context, where levees are not always maintained due to a paucity of funds. Under such circumstances, the approach could be a valid tool for authorities in charge of the levees control. Indeed, the method provides indications on the vulnerability of damaged levees and is a valid tool for prioritizing the maintenance of embanked river stretches as well as for identifying the location where an accurate monitoring is necessary.

The analysis of real conditions of burrows using a 2D and 3D approach by considering geometric conditions closer to the ones observed in the field is the next step of the work.

Acknowledgements

Authors are thankful to Po River Basin Authority, Interregional Agency for the Po River, Magistrate for the Po river and its tributaries, Piedmont Region, Regional Agency for the

Protection of the Environment of Piedmont, Italian National Institute for Environmental Protection and Research and Ministry of the Environment and Protection of Land and Sea for providing the data used for the study. Authors are also grateful to the Editor and anonymous Reviewers for their constructive comments. This work was partly supported by the agreement between the Civil Protection Department and the National Research Council-IRPI.

References

Apel, H., Merz, B. and Thieken, A.H. (2008) Quantification of uncertainties in flood risk assessments. *Journal of River Basin Management*, 6(2), 149-162.

ASCE/EWRI Task Committee on Dam/Levee Breaching (2011) Earthen embankment breaching. *J. Hydr. Eng*, 137(12), 1549–64. DOI:10.1061/(ASCE)HY.1943-7900.0000498.

Barbetta, S., Camici, S., Bertuccioli, P., Palladino, M.R., and Moramarco, T. (2017) Refinement of seepage vulnerability assessment for different flood magnitude in National levee database of Italy. *Hydrology Research - Special Issue Hydrology Days*, 48(3), 763-775, DOI:10.2166/nh.2017.101.

Bardet, J.P., and Tobita, T. (2002) A Practical Method for Solving Free-Surface Seepage Problems. *Computers and Geotechnics*, 29, 451-475.

Bayoumi, A. and Meguid, M.A. (2011) Wildlife and Safety of Earthen Structures: A Review. *Journal of Failure Analysis and Prevention*, 295-319, DOI:10.1007/s11668-011-9439-y, 11(4).

Bendoni, M., Inghilesi, A.F., Mazza, G., Paris, E., Solari, L. and Tricarico, E. (2016) Impact of the invasive red swamp crayfish procambarus clarkii on the seepage processes in river levees. Atti del XXXV Convegno Nazionale di Idraulica e Costruzioni Idrauliche. Bologna, 14-16 settembre 2016.

Borgatti, L., Forte, E., Mocnik, A., Zambrini, R., Cervi, F., Martinucci, D., Pellegrini, F., Pillon, A., Prizzon, A., and Zamariolo, A. (2017) Detection and characterization of animal burrows within river embankments by means of coupled remote sensing and geophysical techniques: Lessons from River Panaro (northern Italy), *Engineering Geology*, 226, 277-289, DOI: 10.1016/j.enggeo.2017.06.017.

Camici, S., Barbetta, S. and Moramarco, T. (2017) Levee body vulnerability to seepage: the case study of the levee failure along the Foenna stream on 1 January 2006 (central Italy). *Journal of Flood Risk Management*, 10, 314-325, DOI:10.1111/jfr3.12137.

Casagrande, A. (1937) Seepage through Dams, Contribution to Soil Mechanics 1925-1940, Boston Society of Civil Engineers, Boston, 1937.

Cheng, H-P., England, S. M. and Murray, C. M. (2016) Seepage and piping through levees and dykes using 2D and 3D modeling codes. Flood and Coastal Storm Damage Reduction Program. Technical report TR-16-6, Engineer Research and Development Center, USACE (US Army Corp of Engineers).

Chlaib, H.K., Mahdi, H., Al-Shukri, H., Su, M.M., Catakli, A., and Abd, N. (2014) Using ground penetrating radar in levee assessment to detect small scale animal burrows. *Journal Applied Geophysics*, 103, 121–131.

Cobos Roa, D. A. (2015) Transient seepage through levees and the influence of roots and animal burrows. Ph.D. dissertation, University of California, Berkeley.

Costa, J.E. (1985) Floods from dam failures. United States Department of Interior Geological Survey, 1-59.

Danka, J., and Zhang, L. M. (2015) Dike failure mechanisms and breaching parameters. *Journal of Geotechnical and Geoenvironmental Engineering*, 141(9), 395-406, DOI:10.1061/(asce)gt.1943-5606.0001335.

Domenico, P.A. and Mifflin, M.D. (1965) Water from low-permeability sediments and land subsidence, Water Resources Research, 1(4), 563-576.

FEMA (2005) FEMA 473-Technical Manual for Dam Owners: Impacts of Animals on Earthen Dams - September 2005.

Huang, W. C., Weng, M. C., Chen, R.K. (2014) Levee failure mechanisms during the extreme rainfall event: a case study in Southern Taiwan, *Nat. Hazard*, 70, 1287-1307, DOI:10.1007/s11069-013-0874-9.

ICOLD (International Commission on Large Dams) (2013) Internal Erosion of Existing Dams, Levees, and Dikes, and Their Foundations, Bulletin 164 Preprint, International Commission on Large Dams, Paris, France.

Jafarzadeh, F., Ferdos, F. and Soleimanbeigi, A. (2009) Comparison between two and three-dimensional seepage analysis of rock-fill dams constructed in narrow valleys - A case study. Commission Internationale des Grands Barrages Brasilia, May 2009.

Kozeny, J. (1931) Grundwasserbewegung bei freiem Spiegel, Fluss-und Kanalversickerung- Nasserkraft und Wasserwirtschaft (Groundwater Movement with Free Surface in Channels and Hydroelectric Energy by Seepage in Channels). Wasserkraft und Wasserwirtschaft, 3, 28-31.

Ludy, J. and Kondolf, G.M. (2012) Flood risk perception in lands "protected" by 100-year levees. *Nat. Hazards*, 61, 829–842, DOI:10.1007/s11069-011-0072-6.

Marchi, E. (1961) Sulla filtrazione attraverso gli argini fluviali. Proceedings of the VII Convegno di Idraulica e costruzioni idrauliche, Palermo (in Italian).

Mazzoleni, M., Barontini, S., Ranzi, R. and Brandimarte, L. (2015) Innovative probabilistic methodology for evaluating the reliability of discrete levee reaches owing to piping, *J. Hydrol. Eng.*, 20(5), DOI:10.1061/(ASCE)HE.1943-5584.0001055.

Michelazzo, G., Paris, E. and Solari, L. (2018) On the vulnerability of river levees induced by seepage, *Journal of Flood Risk Management*, 11, S677-S686, DOI:10.1111/jfr3.12261.

Nagy, L. and Toth, S. (2005) Detailed Technical Report on the collation and analysis of dike breach data with regards to formation process and location factors. Report IMPACT European Project.

Ojha, C.S.P., Singh, V.P. and Adrian, D.D. (2001) Influence of Porosity on Piping Models of Levee Failure, *J. Geotech. Geoenvironmental Eng.*, 127(12), 1071-1074, DOI:10.1061/(ASCE)1090-0241(2001)127:12(1071).

Orlandini, S., Moretti, G. and Albertson, J. D. (2015) Evidence of an emerging levee failure mechanism causing disastrous floods in Italy, *Water Resour. Res.*, 51, 7995–8011, DOI:10.1002/2015WR017426.

Saghaee, G., Meguid, M. A. and Bayoumi, A. (2012) An experimental procedure to study the impact of animal burrows on existing levee structures. Proceedings Eurofuge Conference 2012. Delft, Netherlands. Published by Delft University of Technology and Deltares, DOI:10.4233/uuid:e38ff279-9dd6-4ab4-8517-fac75c19e7fa.

Schultz, M.T., Gouldby, B.P., Simm, J.D. and Wibowo, J.L. (2010) Beyond the factor of safety: developing fragility curves to characterize system reliability. Ed. US Army Corps of Engineers (USACE), Engineer Research and Development Center, Environmental Laboratory, Geotechnical and Structures Laboratory, Vol. 10, 50 pp.

Serre D., Peyras, L., Tourment, R. and Diab, Y. (2008) Levee performance assessment methods integrated in a GIS to support planning maintenance actions, *Journal of Infrastructure Systems*, 14(3), 201-213.

Sills, G.L., Vroman, N.D., Wahl, R.E. and Schwanz, N.T. (2008) Overview of New Orleans levee failures: Lessons learned and their impact on national levee design and assessment, *J. Geotech. Geoenvironmental Eng*. 134, 556–565, DOI:10.1061/(ASCE)1090-0241(2008)134:5(556).

Taccari, M.L. (2015) Study upon the possible influence of animal burrows on the failure of the levee of San Matteo along the Secchia river. MSc Thesis, Delft University of technology, The Netherlands.

Tuller, M. and Or, D. (2004) Water retention and characteristic curve, Chapter in Encyclopedia of soils in the environment, Vol. 4. Ed. By D. Hillel, Elsevier Ltd., Oxford, UK. pp. 278-289.

Van Genuchten, M. (1980) A closed-form equation for predicting the hydraulic conductivity of unsaturated soils, *Soil Science Society of America Journal*, 44, 892-898.

Van Iterson, F. F. (1917) Eenige Theoretische Beschouwinger over Kwel (Some Theoretical Considerations about Seepage), De Ingenieur, 31, 629-633.

Vorogushyn, S., Merz, S. and Apel, H. (2009) Development of dike fragility curves for piping and micro-instability, *Nat. Hazards Earth Syst. Sci*. 9, 1383–1401. DOI:10.5194/nhess-9-1383-2009.

Wu, W., Altinakar, M.S., Al-Riffai, M., Bergman, N., Bradford, S.F., Cao, Z., Chen, Q.J., Constantinescu, Serban G. Duan, J.G., Gee, D.M., Soares-Frazao, S., Song, C.R., Sutherland, J., Teal, M.J., Tsubaki, R., Wahl, T.L., Weston, D.M., Williams, D.T., Zech, Y. and Zhang, L. (2011) Earthen Embankment Breaching, *J. Hydraul. Eng*., 137, 1549–1564. DOI:10.1061/(ASCE)HY.1943-7900.0000498.

Yu, C., Kamboj, S., Wang, C. and Cheng, J.J. (2015) Data Collection Handbook to Support Modeling Impacts of Radioactive Material in Soil and Building Structures. United States – Environmental Science Division, Argonne National Laboratory in US Department of Energy. Web. doi:10.2172/1224969.

WORD COUNT: 5919
(excluding References, Figures, Tables and Appendix A)

APPENDIX A

List of the information sources. For each source, the competent authority providing the data, a synthetic description of the collected data, the data format and the last update are provided. A website link is also reported for the documents which are freely downloadable.

Source	Authority	Data	Format	Updated
Cadastre of the hydraulic works present on the Tanaro river	Magistrate for the Po river and its tributaries	Planimetric configuration of the hydraulic works	Shape files	2002
		Constructive typology, state of efficiency and cross sections of the hydraulic works	Photographs of the sites and data-sheets in pdf format, describing the hydraulic works	
AIPo Institutional website http://geoportale.agenziapo.it/	Interregional Agency for the Po River (AIPo)	Planimetric configuration of the hydraulic works	WMS and Shape files	2012/2013
		Cross sections of the levees at specific locations	xls files	Surveys (1973, 2001, 2005, 2007)
		Flood hazard protection areas	WMS and Shape files	April 2013
Hydrogeological Plan (PAI) Po River Basin	Po River Basin Authority (AdBPo)	Maximum discharges	Tables in pdf format	February 2010
		Flood discharges for fixed return periods: Q_{20}, Q_{100}, Q_{200}, Q_{500}	Tables in pdf format	February 2010
		Water levels profile corresponding to 200 years return period	Tables in pdf format	February 2010
Management Plan of the Hydrographic District of the Po River (PdGPo)	Po River Basin Authority (AdBPo)	Morphological characterization of the river	Data-sheets in pdf format	2015
SICOD, http://www.sistemapiemonte.it/sicod/	Piedmont Region	Planimetric setting and height of the levees, constructive typology and state of efficiency	Shape files	May 2009
Technical reports concerning the hydrological events on the Piedmont territory http://www.regione.piemonte.it/cgi-bin/montagna/pubblicazioni/frontoffice/elenco.cgi?id_settore=10&area=10&argomento=111	Piedmont Region	Hydrological characterization of analysed event, flood-induced damages	Pdf	2016

D.D. 3 december 2012, n. 900 (Piedmont Region regulations) http://www.regione.piemonte.it/ambiente/acqua/atti_doc_adempimenti.htm	Piedmont Region	Thickness of the aquifer	Pdf	2012
Water table depth map http://www.regione.piemonte.it/ambiente/acqua/atti_doc_adempimenti.htm	Piedmont Region	Water table depth from the ground surface	Shape files	2002
Catalog of the peak annual discharges (western Po River Basin) http://www.arpa.piemonte.gov.it/pubblicazioni-2/pubblicazioni-anno-2012/catalogo-delle-portate-massime-annuali-al-colmo-dal-bacino-occidentale-del-po)	Regional Agency for the Protection of the Environment of Piedmont (ARPA)	Maximum water level	Pdf	2012
		Maximum discharge	Pdf	2012
CORINE Land Cover database http://www.sinanet.isprambiente.it/it/sia-ispra/download-mais/corine-land-cover/	ISPRA	Land use	Shape files	2012
Extraordinary plan of remote sensing promoted by the law 179/2002	MATTM, Ministero dell'Ambiente e della Tutela del Territorio e del Mare	1-meter resolution DTM from LIDAR flights	Raster	2009
IRPI historical archive	CNR-IRPI Torino	Documents, Maps and aerial photographs	Paper documents and photographic documents	Variable

FIGURES

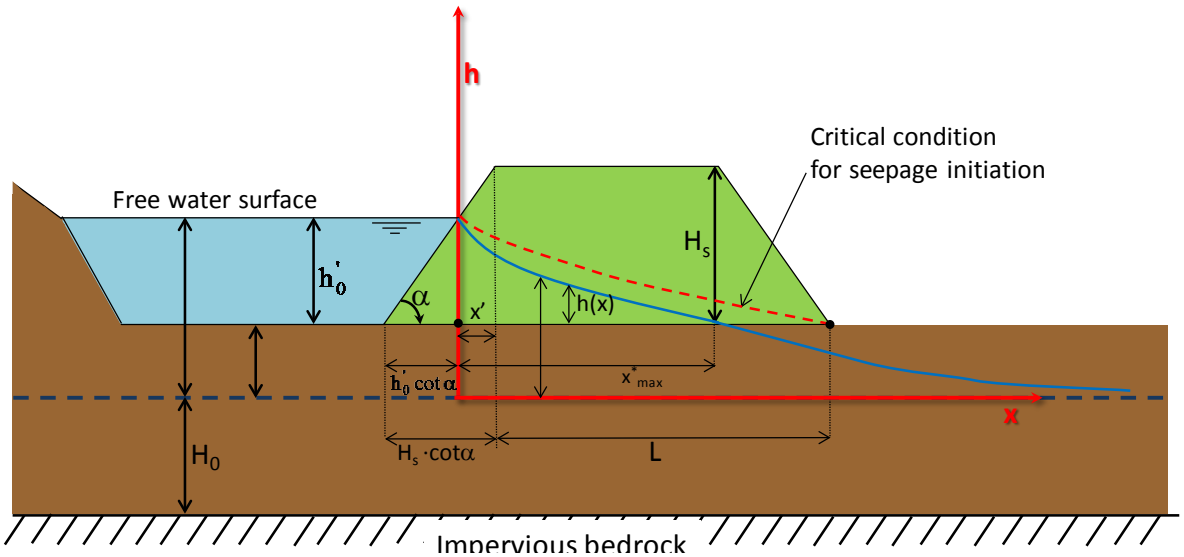

Figure 1*: Scheme of earthen levee and representation of the variables adopted for the definition of the seepage line according to Marchi solution (1961). For symbols, see text. Adapted from Barbetta et al. (2017).*

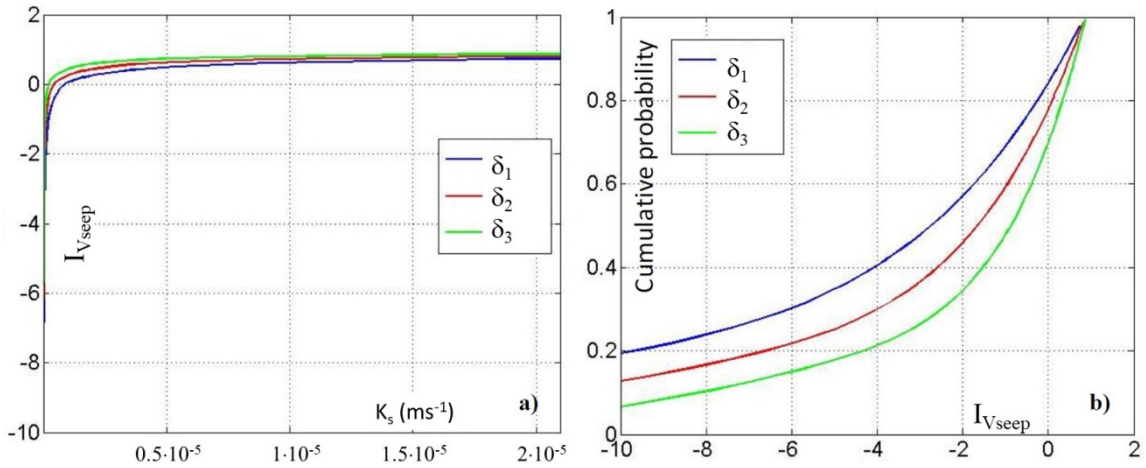

Figure 2 – *Fragility curves for a levee of known geometry (Hs, L, α and H_0) and porosity (ξ) and established flood peak level (h_0'), for different flood durations (D=12, 24 and 48 hours): a) I_{Vseep} as a function of K_s; b) Cumulative probabilities of computed I_{Vseep}.*

a)

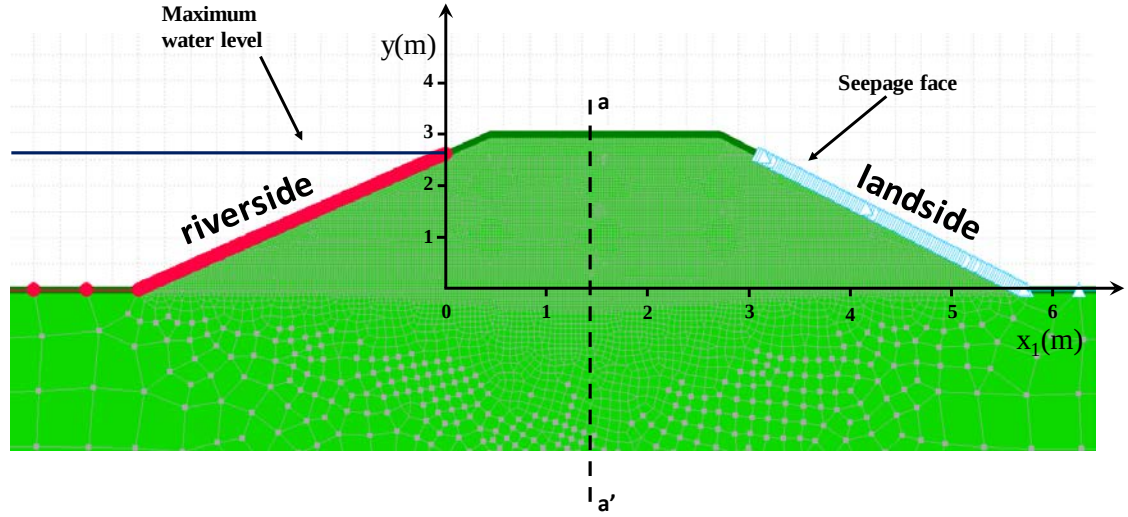

b)

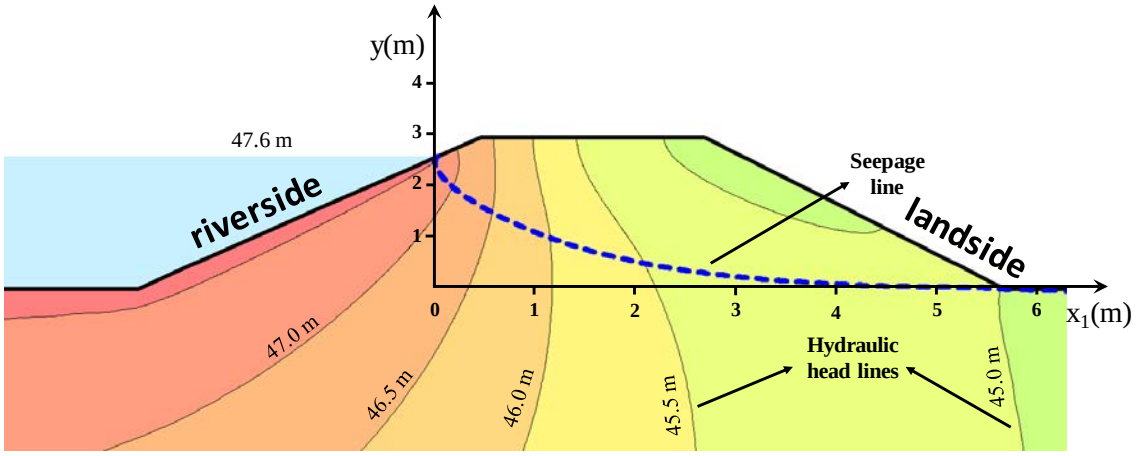

***Figure 3**: Modelling of the undamaged levee in SEEP/W: a) sketch of the seepage domain and established boundary conditions for the transient analysis: a rectangular hydrograph with h_0'=H_{200} is simulated in the river channel; θ_s=0.51m^3/m^3; θ_r=0.102 m^3/m^3;m_v=6·$10^{-5}$$KPa^{-1}$; the black dashed line identifies the vertical section where the total heads distribution is computed and the grey line with red dots identifies the boundary conditions between the river channel and the bare soil both at the riverside and at the river bottom; b) simulation results in terms of hydraulic head contour lines in meter and saturation line.*

a)

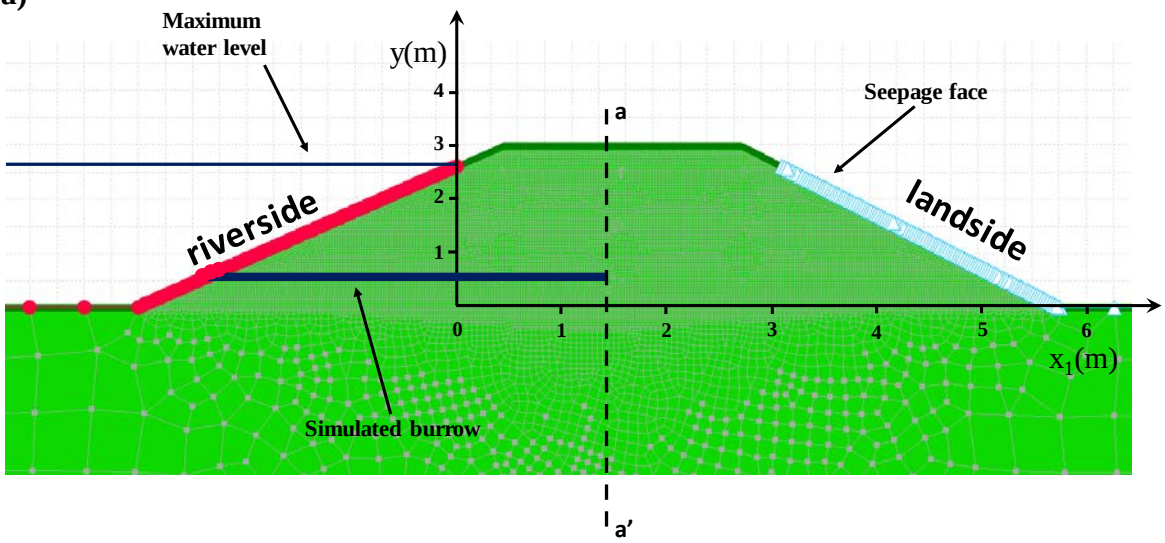

b)

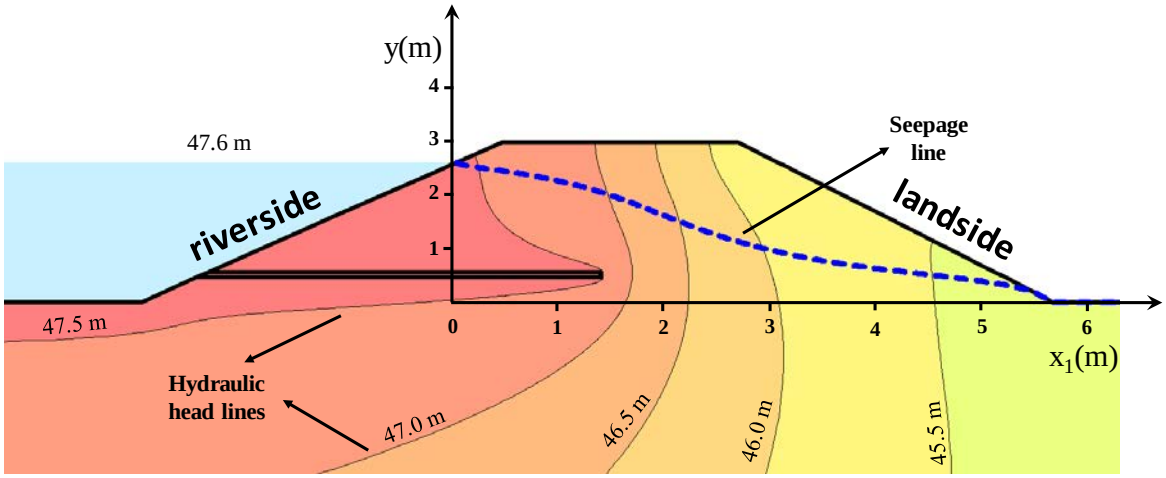

***Figure 4**: Modelling of the levee affected by burrow in SEEP/W (GEOSTUDIO® 2012 Office): a) sketch of the seepage domain, hypothesised burrow and established boundary conditions for the transient analysis: a rectangular hydrograph with h_0'=H_{200} is simulated in the river channel; θ_s=0.51m^3/m^3; θ_r=0.102 m^3/m^3;m_v=6·$10^{-5}KPa^{-1}$; the black dashed line identifies the vertical section where the total heads distribution is computed; b) simulation results in terms of hydraulic head contour lines in meter.*

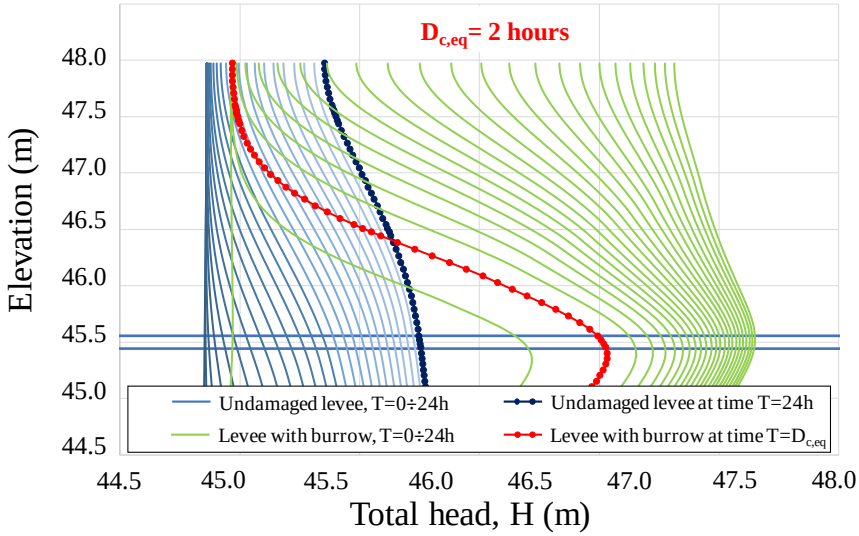

***Figure 5**: Evolution of the total head profiles across the vertical section crossing the centreline of the levee: 1) light blue lines=total heads in the intact levee, for hourly time steps in the interval 0÷T=24 hours; 2) green lines=total heads in the levee with burrow, for hourly time steps in the interval 0÷T=24 hours; 3) dark blue line=total head profile in the undamaged levee, corresponding to a flood duration T=24 hours; 4) red line=total head profile in the damaged embankment, for a flood duration equal to the equivalent critical duration, $D_{c,eq}$=2 hours.*

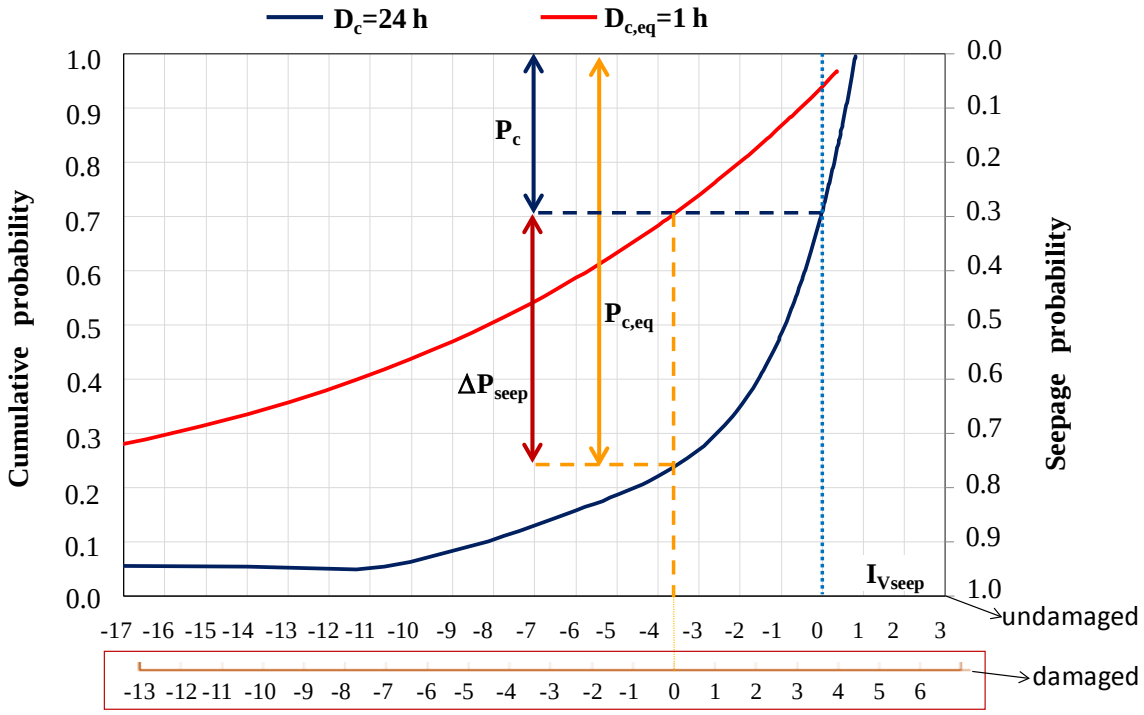

***Figure 6**: Seepage probability variation induced by the presence of the burrow in the levee, ΔP_{seep}. The fragility curves refer to an undamaged levee and are estimated by the expeditious procedure (Barbetta et al., 2017). The upper I_{Vseep} axis is referred to the undamaged levee, while the lower axis is referred to the damaged one.*

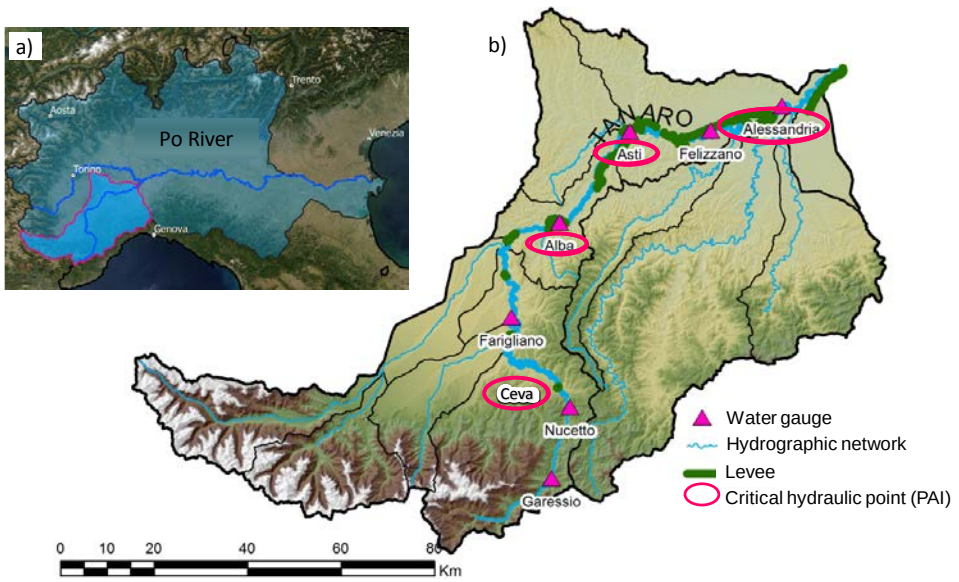

***Figure 7**: Tanaro River basin. a) Location within the Po River catchment. b) Location of the relevant hydraulic elements: main river network (light blue lines), earthen levees as reported in the Information System realized by the Piedmont Region (green lines), critical hydraulic points (circled*

in fuchsia) and water gauges (fuchsia triangles) identified by the Hydro-geological Arrangement Plan of the Po River.

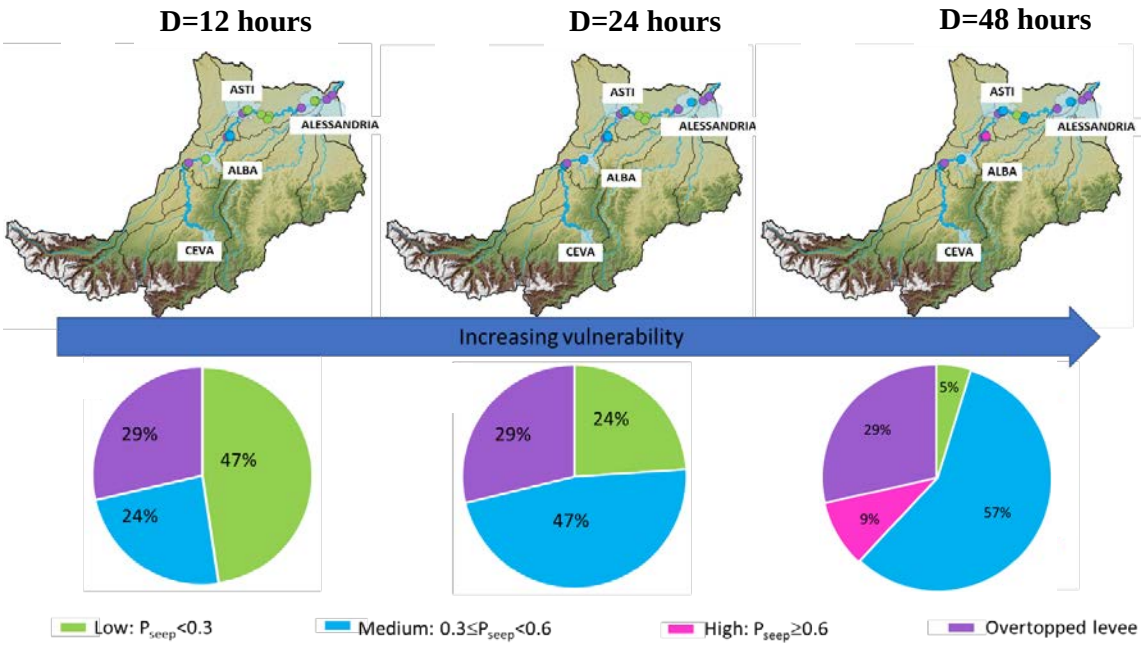

***Figure 8**: Location of the investigated levees and associated distribution of the seepage vulnerability classes for different flood durations (D=12, 24 and 48 hours), in the hypothesis of undamaged structures.*

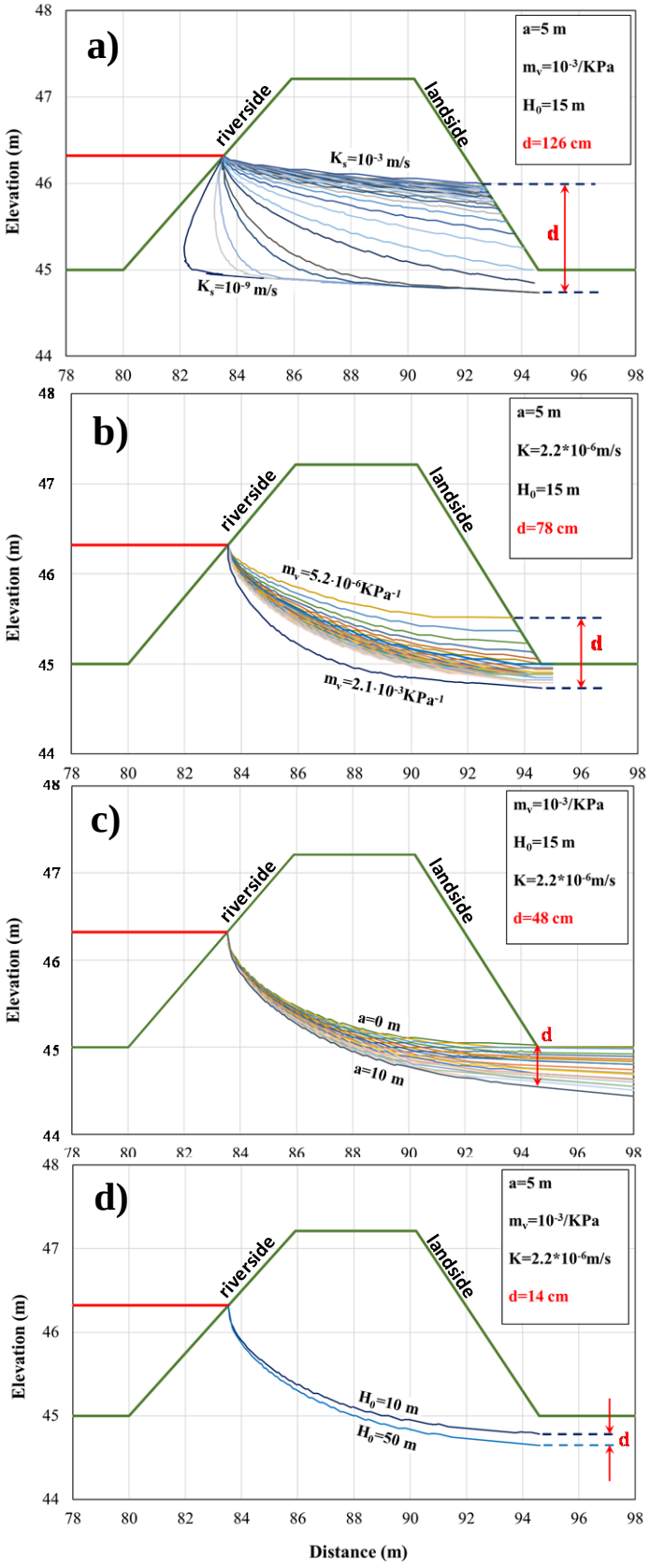

***Figure 9**: Sensitivity of the seepage line to the geotechnical and geometrical parameters used in SEEP/W simulations: a) soil hydraulic conductivity, K_s; b) soil volumetric compressibility, m_v; c) water table depth, a; d) thickness of the aquifer, H_0.*

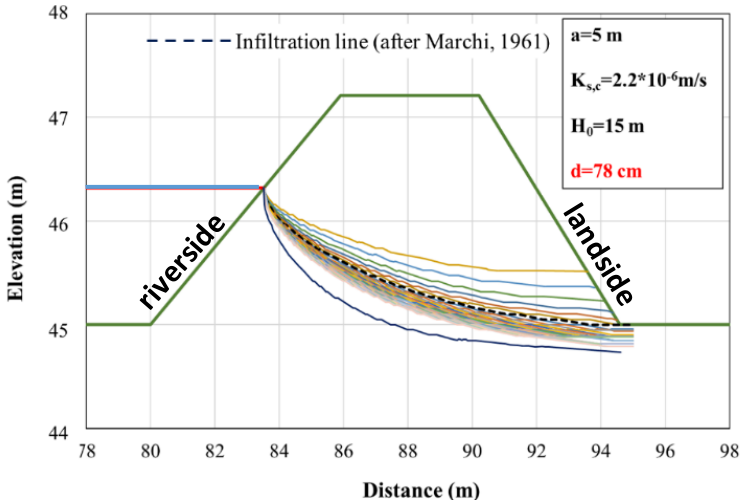

***Figure 10**: Comparison between the seepage line provided by the formulation of Marchi (1961) (black, dashed line) and the ones provided by SEEP/W for different m_v values (coloured, solid lines).*

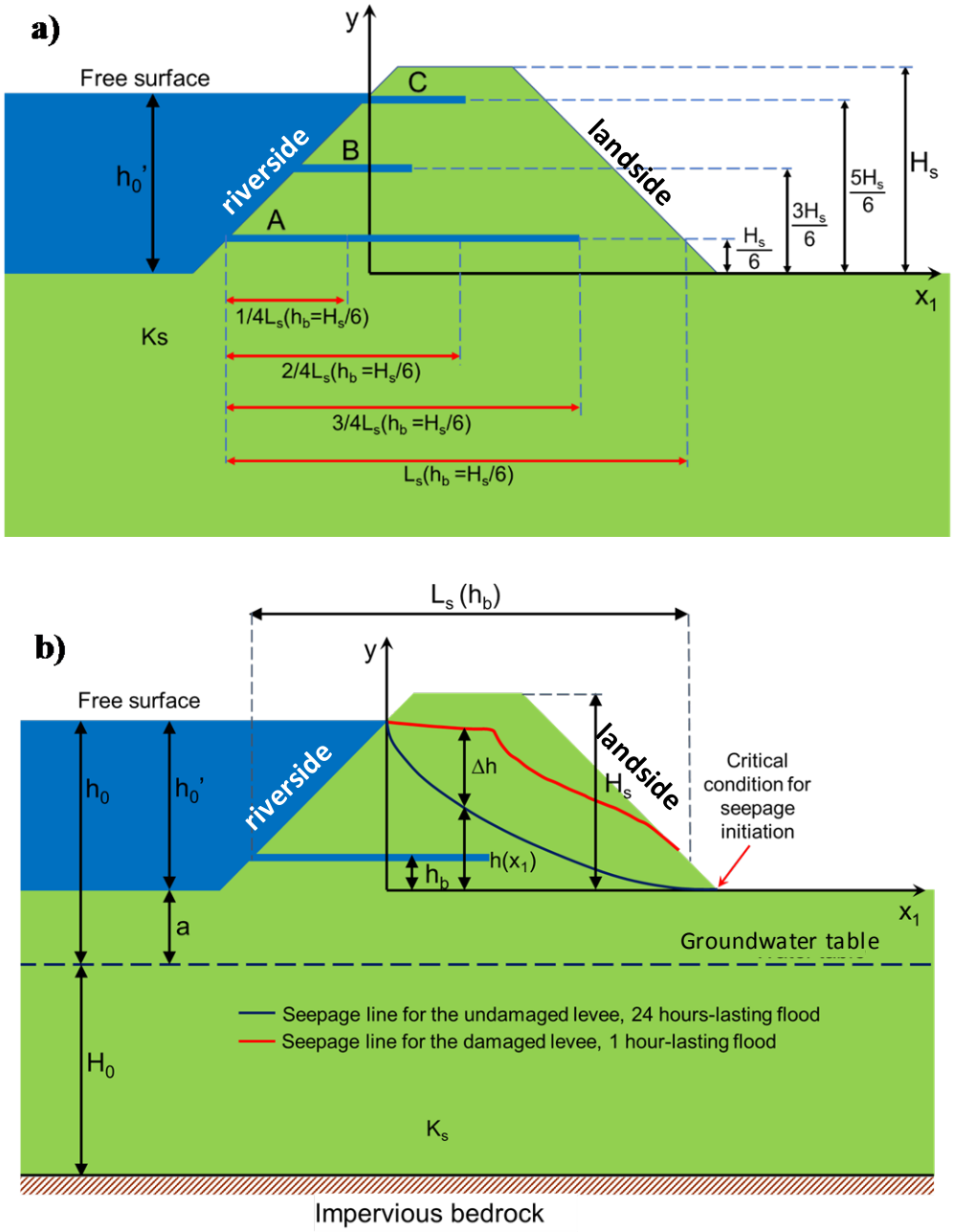

***Figure 11**: Analysis of the effect of burrows in earthen levees: a) burrow configurations analysed with SEEP/W; b) modification of the seepage line induced by the burrow (blue solid line=seepage line in the undamaged levee after the 24 hours-lasting flood; red solid line= seepage line in the damaged levee, after the 1 hour-lasting flood).*

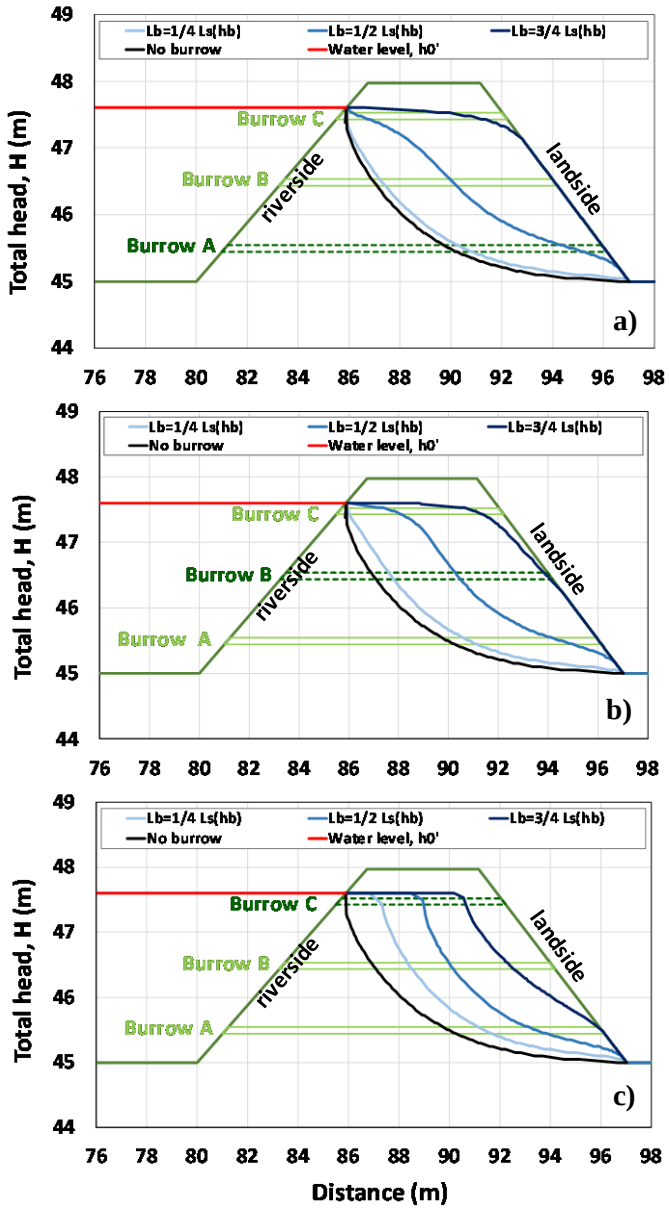

***Figure 12**: Seepage line modifications due to the burrows, for different locations and lengths of the cavities: a) Burrow A: $h_b=1/6H_s$; b) Burrow B: $h_b=1/2H_s$; c) Burrow C: $h_b=5/6H_s$. For each location, three possible lengths are analysed: $L_b=1/4L_s(h_b)$, $1/2L_s(h_b)$ and $3/4L_s(h_b)$.*

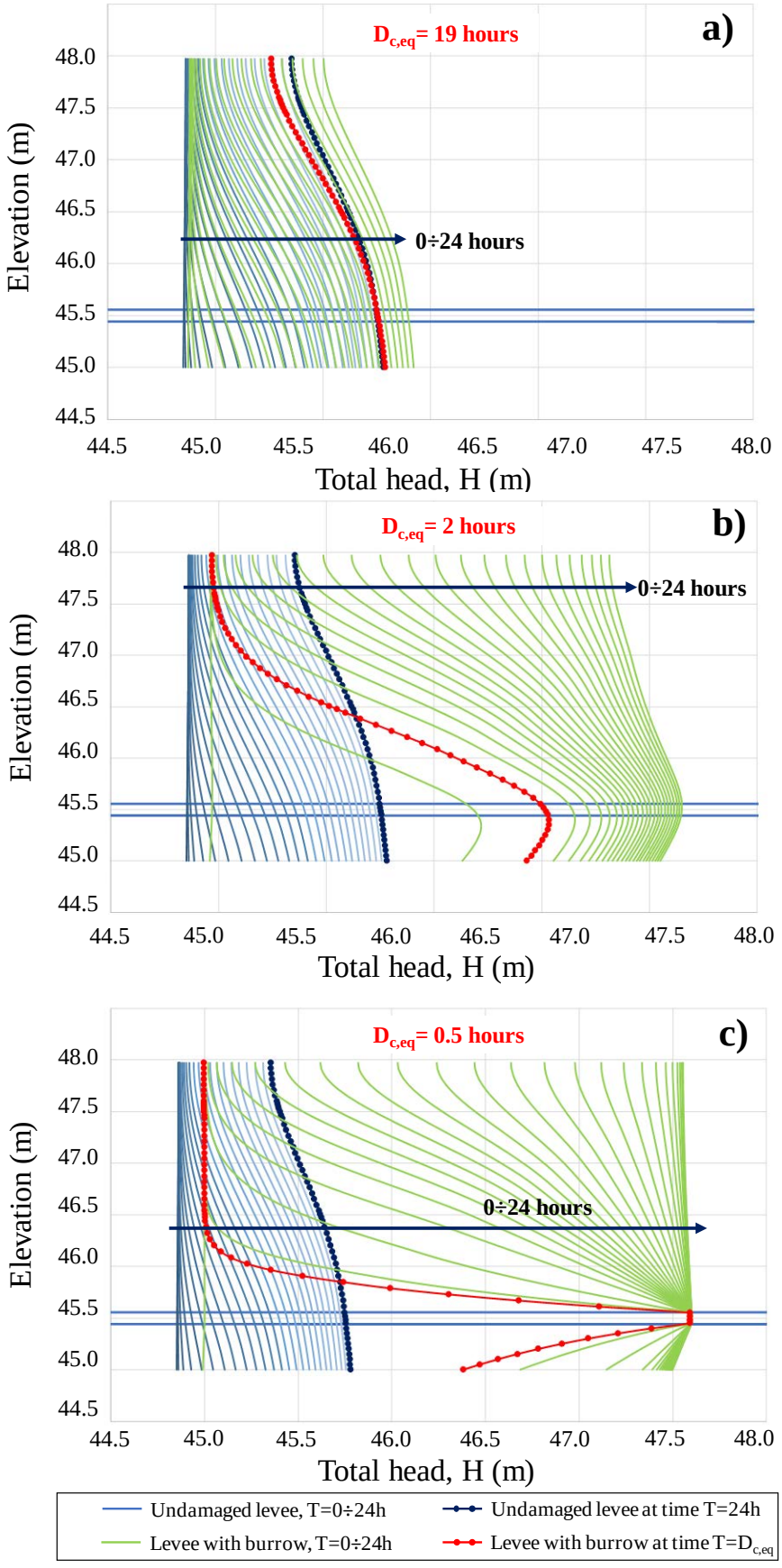

***Figure 13**: Total heads profiles corresponding to the vertical section crossing the centreline of the levee Ta_07_dx for burrow in A position (h_b=1/6H_s) and increasing lengths of the cavity: a) L_b=1/4L_s(h_b); b) L_b=1/2 L_s(h_b); c) L_b=3/4 L_s(h_b).*

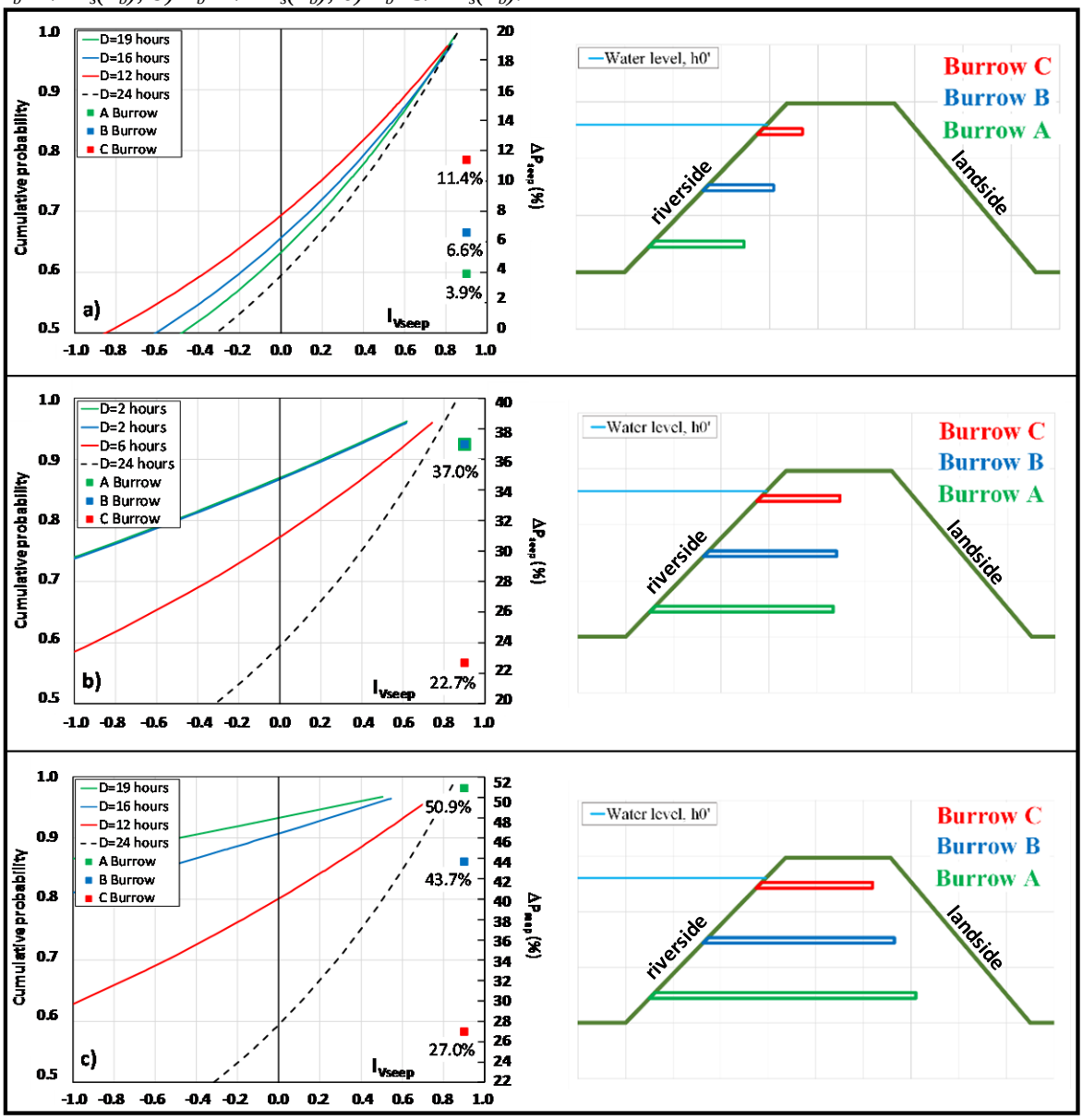

***Figure 14**: Seepage probability variation induced by the burrows in the Ta_07_dx levee, for different configurations of the cavities: a) burrow (A, B or C) with L_b=1/4L_s(h_b); b) burrow (A, B or C) with L_b=1/2L_s(h_b); c) burrow (A, B or C) with L_b=3/4L_s(h_b).*

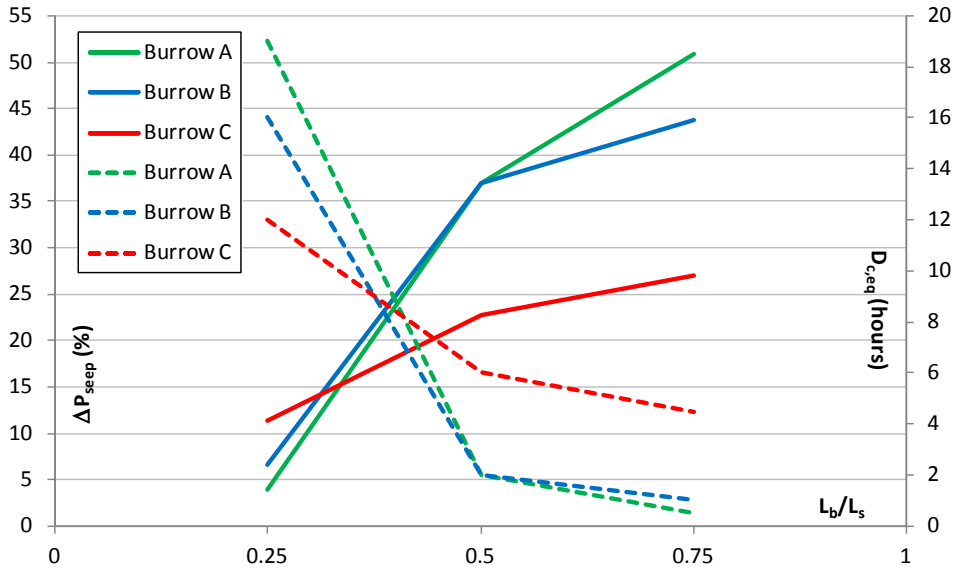

***Figure 15**: Effect of the burrows for Ta_07_dx levee, in terms of critical equivalent durations, $D_{c,eq}$, reduction (dashed coloured lines) and percentage seepage probability variation, ΔP_{seep} (%) (solid coloured lines) for different locations and lengths of the cavities.*

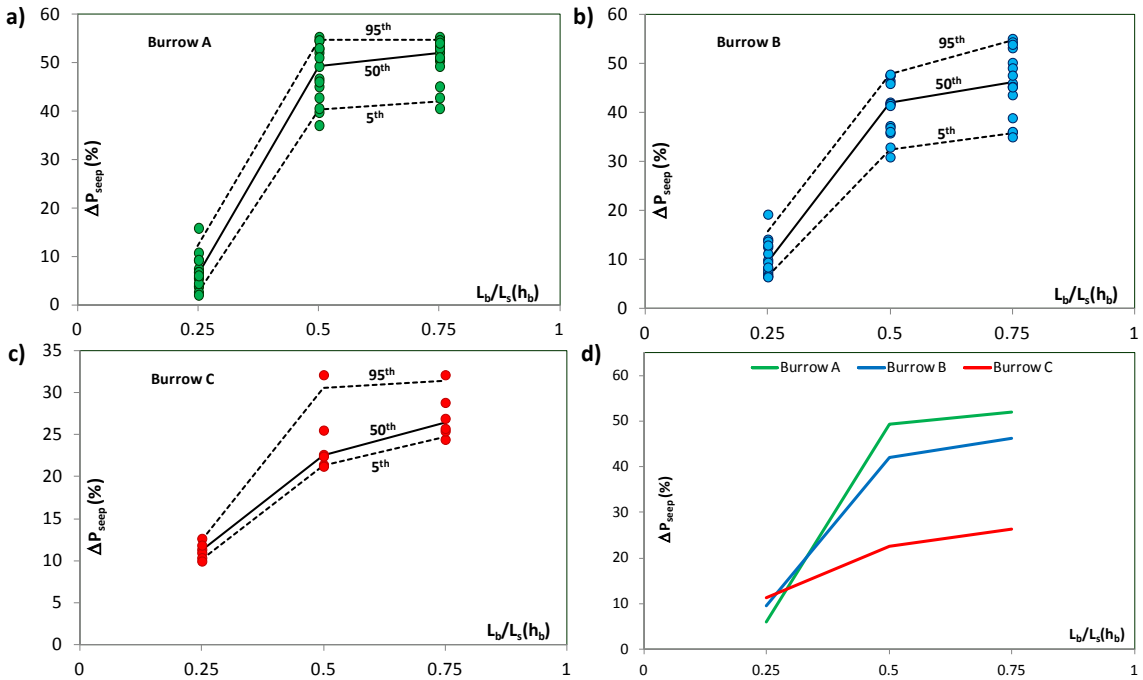

***Figure 16**: Tanaro River levees: percentage seepage probability variation, due to the burrows. ΔP_{seep} (%) computed for each levee are shown along with the 5th, 50th and 95th percentiles for: a) burrow A; b) burrow B; c) burrow C. The 50th percentiles are compared in figure d).*

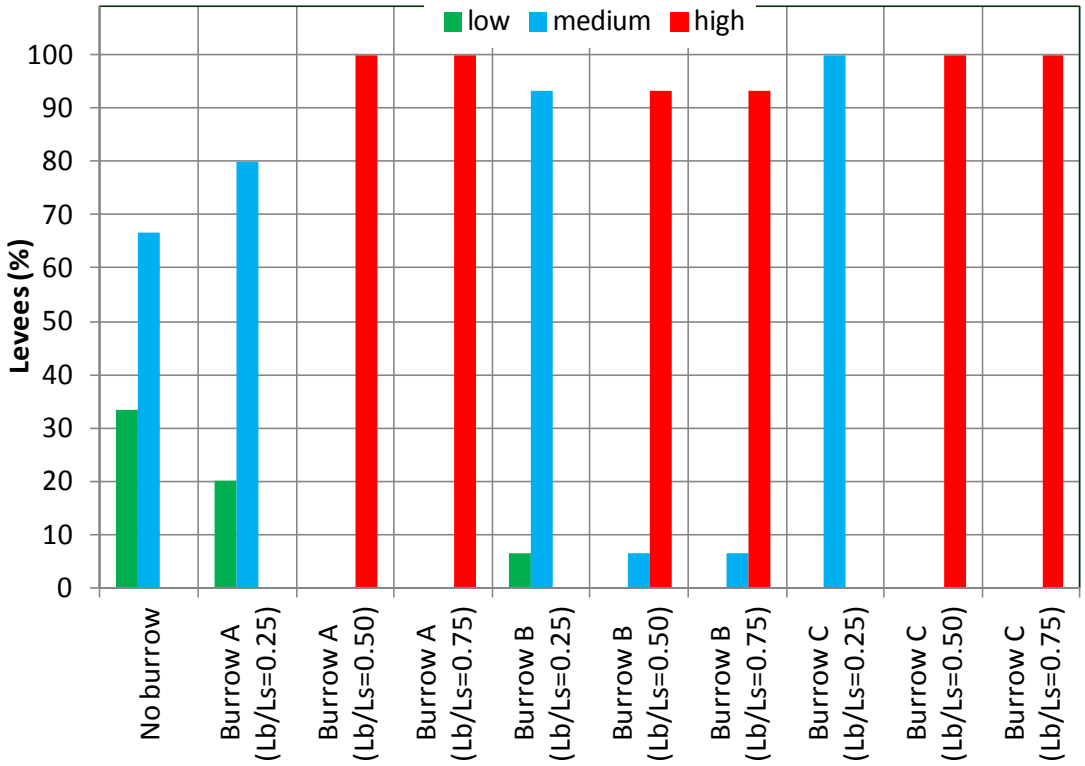

***Figure 17**: Tanaro levee database: vulnerability classes distribution for undamaged structures (no burrow) and levees affected by burrows, for different locations (A: $h_b=1/6H_s$; B: $h_b=1/2H_s$; C: $h_b=5/6H_s$) and different lengths ($L_b=1/4$, 1/2 and $3/4L_s(h_b)$).*

TABLES

***Table 1**: Seepage vulnerability classes according to Barbetta et al. (2017).*

Seepage Probability <0.3	0.3 ≤ Seepage Probability <0.6	Seepage Probability ≥0.6
Low vulnerability	Medium vulnerability	High vulnerability

***Table 2**: Tanaro River: main characteristics of the levees (levee height, H_s, levee width, B, crown width, b, landside slope, ϑ, riverside slope, α). The water level for a return period of 200 years, H_{200}, is shown along with the seepage probability, P_{seep}, and vulnerability class estimated for undamaged levee and flood durations D=12, 24 and 48 hours (L=Low vulnerability, M=Medium vulnerability, H=High vulnerability).*

Levee code (levee side)	H_s (m)	B (m)	b (m)	ϑ	α	H_{200} (m)	P_{seep} (vulnerability class)		
							D=12 hs	D=24 hs	D=48 hs
Ta_01_sx (left)	2.89	16.47	6.42	40.12	23.45	2.46	0.3069 (M)	0.402 (M)	0.5149 (M)
Ta_02_sx (left)	2.53	16.84	6.06	27.18	23.47	1.91	0.2475 (L)	0.316 (M)	0.4059 (M)
Ta_03_sx (left)*	1.83	15.39	5.34	20.98	19.11	1.85	Overtopped		
Ta_04_dx (right)	2.93	13.89	4.03	26.04	36.20	1.71	0.2574 (L)	0.322 (M)	0.4257 (M)
Ta_05_sx (left)*	1.38	5.27	0.90	37.26	28.25	2.9	Overtopped		
Ta_06_sx (left)	3.34	15.96	4.88	29.09	31.63	2.6	0.2871 (L)	0.360 (M)	0.4851 (M)
Ta_07_dx (right)	2.97	17.01	4.42	26.06	23.35	2.6	0.3168 (M)	0.405 (M)	0.5149 (M)
Ta_08_dx (right)*	2.73	16.65	4.48	24.09	23.70	4.2	Overtopped		
Ta_09_dx (right)	2.74	14.45	3.54	27.28	25.99	2.4	0.3564 (M)	0.505 (M)	0.6436 (H)
Ta_10_sx (left)	2.67	17.08	6.6	24.08	30.42	1.7	0.2178 (L)	0.260 (L)	0.3465 (M)
Ta_11_sx (left)	2.3	15.54	5.34	24.87	22.65	1.9	0.2871 (L)	0.400 (M)	0.4851 (M)
Ta_12_sx (left)	3.62	20.48	4.66	21.50	27.52	2.7	0.2178 (L)	0.275 (L)	0.3465 (M)
Ta_13_sx (left)*	2.23	11.72	3.59	25.97	30.70	3.2	Overtopped		
Ta_14_dx (right)	2.21	20.21	9.97	21.65	24.25	1.74	0.2079 (L)	0.2555 (L)	0.3465 (M)
Ta_15_sx (left)	2.77	14.82	5.56	30.33	29.47	2.0	0.2772 (L)	0.350 (M)	0.4752 (M)
Ta_16_sx (left)*	2.42	18.08	3.65	19.63	17.36	3.8	Overtopped		
Ta_17_dx (right)*	2.88	17.35	4.89	23.50	26.56	3.14	Overtopped		
Ta_18_dx (right)	3.01	16.80	3.58	23.83	25.23	2.71	0.3366 (M)	0.425 (M)	0.5644 (M)
Ta_19_dx (right)	2.51	14.35	3.38	22.56	27.05	2.39	0.3465 (M)	0.490 (M)	0.6337 (H)
Ta_20_sx (left)	6.14	35.56	4.92	19.39	25.03	4.48	0.1089 (L)	0.165 (L)	0.2376 (L)
Ta_21_dx (right)	2.21	14.59	4.31	27.16	20.19	1.32	0.2277 (L)	0.29 (L)	0.3564 (M)
*: overtopped levee									

***Table 3**: Representative values of saturated hydraulic conductivity of different soil materials (Yu et al., 2015).*

Texture	Saturated Hydraulic Conductivity, K (m/yr)
Sand	5.55×10^3
Loamy sand	4.93×10^3
Sandy loam	1.09×10^3
Silty loam	2.27×10^2
Loam	2.19×10^2
Sandy clay loam	1.99×10^2
Silty clay loam	5.36×10
Clay loam	7.73×10
Sandy clay	6.84×10
Silty clay	3.21×10
Clay	4.05×10

***Table 4**: Typical values for the residual (θ_r) and saturated (θ_s) volumetric water contents and for the Van Genuchten model parameters, α and n (Van Genuchten, 1980), for different textural classes, deduced by Tuller and Or (2004).*

Textural class	N	θ_r ($cm^3\ cm^{-3}$)	θ_s ($cm^3\ cm^{-3}$)	α (cm^{-1})	n
Sand	126	0.058	0.37	0.035	3.19
Loamy sand	51	0.074	0.39	0.035	2.39
Sandy loam	78	0.067	0.37	0.021	1.61
Loam	61	0.083	0.46	0.025	1.31
Silt	3	0.123	0.48	0.006	1.53
Silt loam	101	0.061	0.43	0.012	1.39
Sandy clay loam	37	0.086	0.40	0.033	1.49
Clay loam	23	0.129	0.47	0.030	1.37
Silty clay loam	20	0.098	0.55	0.027	1.41
Silty clay	12	0.163	0.47	0.023	1.39
Clay	25	0.102	0.51	0.021	1.20

N, the number of soils or samples of a given textural class from which the mean values are compiled.
Reproduced from Leij FJ, Alves WJ, van Genuchten MT, and Williams JR (1996) *The UNSODA Unsaturated Hydraulic Database*. EPA/600/ R-96/095. Cincinnati, OH: US Environmental Protection Agency.

***Table 5**: Range of m_v values for various natural soils (Domenico and Mifflin, 1965).*

Soil type	Volumetric compressibility, m_v (KPa^{-1})
Plastic clay	2.1·10-3 ÷ 2.6·10-4
Stiff clay	2.6·10-4 ÷ 1.3·10-4
Medium hard clay	1.3·10-4 ÷ 6.9·10-5
Loose sand	1.0·10-4 ÷ 5.2·10-5
Dense sand	2.1·10-5 ÷ 1.3·10-5
Dense sandy gravel	1.0·10-5 ÷ 5.2·10-6

***Table 6**: Sensitivity of the seepage line to the parameters used in SEEP/W analyses, expressed as a function of the seepage line excursion at the landside toe of the levee, d.*

Parameter (Units)	**Source of information**	**Range of variation**	**Vertical excursion of seepage line at the landward levee toe, d (cm)**
K_s (m/s)	USACE, 1993	$10^{-9} \div 10^{-3}$	126
m_v (KPa^{-1})	Domenico and Mifflin, 1965	$2.1x10^{-3} \div 5.2x10^{-6}$	78
a (m)	Water table depth map	0 ÷ 10	48

	(Piedmont Region)		
H_0 (m)	Piedmont Region regulations	10 ÷ 50	14

***Table 7**: Ranges of variation of the equivalent critical durations deduced for the Tanaro River levees, for all the possible configurations of the burrow (for symbols see text).*

Burrow	**Location**	**L_b=¼ L_s**	**L_b= ½ L_s**	**L_b= ¾ L_s**
		$D_{c,eq}$ (hours)	**$D_{c,eq}$ (hours)**	**$D_{c,eq}$ (hours)**
A	(1/6 H_s)	8.5 - 19.0	0.5 - 1.5	0.5 - 1.0
B	(3/6 H_s)	7.0 - 16.5	1.0 - 2.0	0.5 - 1.5
C (*)	(5/6 H_s)	9.5 - 13.5	2.5 - 6.5	2.5 - 5.0
(*) C burrow is analysed only for 6 levees out of 15				

***Table 8**: Seepage probabilities computed for the Tanaro levees, for different surmised burrow locations (A: h_b=1/6Hs; B: h_b=1/2H_s and C: h_b=5/6H_s) and burrow lengths (L_b=1/4,1/2 and 3/4L_s(h_b)). The equivalent durations, $D_{c,eq}$, (in hours) and the vulnerability classes (L=low, M=medium, H=high) of the damaged structures are reported in brackets and can be compared with the vulnerability class of the intact structures for D_c=24 (No burrow).*

Levee code	**No burrow**		**L_b=1/4L_s(h_b)**			**L_b=1/2L_s(h_b)**			**L_b=3/4L_s(h_b)**		
			A	**B**	**C**	**A**	**B**	**C**	**A**	**B**	**C**
	P_c	**Vulnerability class**	**$P_{c,eq}$ ($D_{c,eq}$ (hours); Vuln. class)**			**$P_{c,eq}$ ($D_{c,eq}$ (hours); Vuln.**			**$P_{c,eq}$ ($D_{c,eq}$ (hours); Vuln.**		
Ta_01_sx	40.2%	M	43.9% (19;M)	47.4% (15;M)	52.9% (11;M)	79.9% (1.5;H)	77.6% (2;H)	65.8% (5;H)	90.5% (0.5;H)	90.5% (0.5;H)	69.1% (4;H)
Ta_02_sx	31.6%	M	37% (16.5;M)	41.6% (12;M)	-	78.2% (1;H)	78.2% (1;H)	-	84.9% (0.5;H)	84.9% (0.5;H)	-
Ta_04_dx	32.2%	M	48% (8.5;M)	51.5% (7;M)	-	85% (0.5;H)	74.4% (1.5;H)	-	85% (0.5;H)	78.3% (1;H)	-
Ta_06_sx	36.0%	M	45.2% (13.5;M)	48.6% (11;M)	-	88% (0.5;H)	77.9% (1.5;H)	-	88% (0.5;H)	81.4% (1;H)	-

Ta_07_dx	40.5%	M	44.4% (19;M)	47.1% (16;M)	51.9% (12;M)	77.5% (2;H)	77.5% (2;H)	63.2% (6;H)	91.4% (0.5;H)	84.2% (1;H)	67.5% (4.5;H)
Ta_09_dx	50.0%	M	55.6% (18;M)	58.3% (15.5;M)	61% (13;H)	95% (0.5;H)	83% (2;H)	71.5% (6.5;H)	95% (0.5;H)	86.1% (1.5;H)	74.5% (5;H)
Ta_10_sx	26.0%	L	36.7% (10.5;M)	40.2% (8.5;M)	-	81.2% (0.5;H)	73.6% (1;H)	-	81.2% (0.5;H)	81.2% (0.5;H)	-
Ta_11_sx	40.0%	M	42.6% (17;M)	47.7% (12.5;M)	51.9% (9.5;M)	89.2% (0.5;H)	81.9% (1;H)	72.2% (2.5;H)	89.2% (0.5;H)	89.2% (0.5;H)	72.2% (2.5;H)
Ta_12_sx	27.5%	L	34.9% (13.5;M)	38.8% (10.5;M)	-	82% (0.5;H)	75.2% (1;H)	-	82% (0.5;H)	75.2% (1;H)	-
Ta_14_dx	25.5%	L	32.2% (13.5;M)	35% (11;M)	-	80% (0.5;H)	73.4% (1;H)	-	80% (0.5;H)	80% (0.5;H)	-
Ta_15_sx	35.0%	M	44.2% (13.5;M)	48,8% (10;M)	-	87.9% (0.5;H)	76.5% (1.5;H)	-	87.9% (0.5;H)	80.3% (1;H)	-
Ta_18_dx	42.5%	M	46.9% (18;M)	49.3% (16;M)	52.9% (13;M)	85.2% (1;H)	78.4 (2;H)	63.8% (6.5;H)	85.2% (1;H)	81.5% (1.5;H)	68% (5;H)
Ta_19_dx	49.0%	M	55.7% (16.5;M)	57.5% (15;M)	59% (13.5;M)	89.5% (1;H)	85.2% (1.5;H)	71.5% (6;H)	89.5% (1;H)	85.2% (1.5;H)	74.8% (4.5;H)
Ta_20_sx	16.5 %	L	18.5% (15;L)	23% (12;L)	-	67.5% (0.5;H)	47.5% (2;M)	-	67.5% (0.5;H)	51.6% (1.5;M)	-
Ta_21_dx	29.0%	L	35% (15;M)	42% (9.5;M)	-	75% (1;H)	75% (1;H)	-	83% (0.5;H)	83% (0.5;H)	-